博士学位論文

Mg-dechelatase Encoded by Chlamydomonas *Stay-Green* is Involved in the Formation of Photosystem II but not in Chlorophyll Degradation

（Stay-Green 遺伝子の産物 Mg-脱離酵素はクラミドモナスではクロロフィルの分解ではなく光化学系 II の形成に関与する）

Chen Ying

北海道大学大学院生命科学院

2019 年 3 月

Contents

Abstract

Pheophytin (Pheo) *a* is an indispensable molecule in photosystem (PS) II, and is a product in the first step of Chlorophyll (Chl) degradation as well. So, it is seemingly suggested that the *STAY-GREEN* (*SGR*) gene, which encodes an Mg-dechelatase that catalyzes the conversion of Chl *a* to Pheo *a*, is involved in both the formation of PSII and the degradation of Chl. In this study, a series of experiments were carried out to investigate the physiological functions of Chlamydomonas *SGR*.

Two Chlamydomonas *sgr* null mutants were prepared by screening an insertion-mutant library. The Fv/Fm ratios of wild type (WT), *sgr* mutants, and complementations under several light conditions were observed. The lower Fv/Fm ratios of *sgr* mutants suggested a lower PSII activity. High-performance liquid chromatography (HPLC) analysis showed reduced Pheo *a*/Chl levels of *sgr* mutants, implying a reduced PSII levels. The growth rates in the presence (TAP medium) and absence (HSM medium) of a carbon source were examined. The *sgr* mutants exhibited reduced photomixotrophical and photoautotrophic growth rate. Blue-native polyacrylamide gel electrophoresis (BN-PAGE) and immunoblotting analysis showed the PSII levels were reduced in *sgr* mutants, with PSI and LHCII levels unchanged. The reduced PSII levels were verified by low-temperature fluorescence spectroscopy of whole cells. These results indicate that Chlamydomonas *SGR* is involved in PSII formation.

In Nitrogen (N) starvation under both photomixotrophic and photoautotrophic conditions, Chl degradation proceeded in the *sgr* mutants as in WT. The qRT-PCR results presented that the expression level of SGR kept unchanged during N starvation. These results indicate that *SGR* is not required for Chl degradation.

Compare with Arabidopsis WT, *sgr 1 2 l* triple mutant, a mutant with the complete absence of SGR activity, showed similar growth speed and Fv/Fm ratio at the developmental stage. Immunoblotting analysis showed that the proteins in PSs and LHCII of *sgr* triple mutants were normally synthesized at the developmental stage. HPLC analysis showed similar pigments levels in Arabidopsis WT and *sgr* triple

mutant at the developmental stage. BN-PAGE results demonstrated PS SC of *sgr* triple mutants were normally assembled at the developmental stage but less disassembled at senescence stage. At senescence stage, *sgr* triple mutants showed stay green phenotype and reduced Fv/Fm ratios. These results indicate Arabidopsis *SGR* participates in Chl degradation but not in PSII formation.

According to the above results, Chlamydomonas *SGR* is involved in PSII formation but not in Chl degradation.

Keywords

Arabidopsis
Chlamydomonas
chlorophyll *a*
chlorophyll degradation
Mg-dechelatase
pheophytin *a*
photosynthesis
photosystem II formation
senescence
STAY-GREEN

Abbreviations

BN-PAGE	blue native polyacrylamide gel electrophoresis
Chl	chlorophyll
Fv/Fm	maximum quantum efficiency of PSII
HPLC	high performance liquid chromatography
LHCII	light-harvesting Chl *a*/*b* complex
LMM	low molecular mass
OEC	oxygen evolving complex
Pheo	pheophytin
PS	photosystem
qRT-PCR	real-time polymerase chain reaction
RC	reaction center
SDS-PAGE	sodium dodecyl sulphate-polyacrylamide gel electrophoresis
SGR	STAY-GREEN
TAIL	thermal asymmetric interlaced
2D-PAGE	two-dimensional gel electrophoresis

1. Introduction

1.1. Oxygenic Photosynthesis.

Oxygenic photosynthesis occurs in certain types of cyanobacteria, algae, and plants, which can fix photochemistry energy and CO_2 into biological energy, accompanying with water splitting to generate O_2 (Cogdell et al., 2012). Oxygenic photosynthesis encompasses two major stages——energy-transduction reactions ("light-dependent reactions") and carbon-fixation reactions ("light-independent reactions") (Cowgill et al., 2012).

In "light-dependent reactions", light energy is captured by the light-harvesting complex (LHC) and delivered to photosystem (PS) II reaction center (RC) that contains special chlorophyll (Chl) molecules named P680. P680 boosts an electron to a high energy level. This electron is passed to an acceptor molecule and replaced with an electron from water to release O_2. (Hohmann-Marriott and Blankenship, 2011). The released electron who come from water is transferred to a dimer of Chl *a* molecule in PSI named P700. The electron in P700 is boosted to a high energy level and transferred to an acceptor molecule. The net effect of the "light-dependent reactions" is the production of adenosine triphosphate (ATP) and triphosphopyridine nucleotide (NADPH) that can be used in the "light-independent reactions" (Hügler and Sievert, 2011). "light-independent reactions" involves a series of reactions including carbon fixation, reduction, and regeneration of the ribulose 1,5-bisphosphate (RuBP). These reactions can be executed by four multiunit membrane-protein complexes located in the chloroplast thylakoid membranes called PSs.

1.2. Photosystem.

PSs including PSI as a plantacyanin-ferredoxin oxidoreductase, PSII as a water-plastoquinone oxidoreductase, cytochrome (Cyt) $b_{559}f$ as a plastoquinone-plastoquinone oxidoreductase, and ATP synthase (ATPase) as a pmf-driven ATPase (Rev et al., 2000; Nelson and Ben-Shem, 2004). Both PSs containing multiple subunits, pigments, redox cofactors, associated with their antenna systems. Both PSs are synthesized through the coordinate process of the nuclear and chloroplast genetic systems (Nelson and Junge, 2015).

1.2.1. PSII.

In algae and plants, PSII contains more than 20 subunits and approximately 80 cofactors, including a RC that is the site of the initial electron transfer reactions, an Mn_4O_xCa cluster that catalyzes water oxidation, a binding pocket for the reduction of plastoquinone, and a peripheral antenna system that employs Chl and other pigment molecules to absorb light. The proteins could be classified into four groups as follows: PSII core proteins, low-molecular-mass (LMM i.e., <10-kDa) proteins, extrinsic oxygen-evolving complex (OEC) proteins, and LHCII proteins.

The highly conserved PSII RC core as the minimal set of subunits are present in the heterodimer (or oligomer). The heterodimer of PSII RC core consists of about 35 Chls and more than 20 intrinsic and extrinsic proteins (Umena et al., 2011). D1 (32-kDa, chloroplast *psb*A gene product) and D2 (34-kDa, chloroplast *psb*D gene product) (Shen, 2015) polypeptides compose the heterodimer protein complex as the key redox components. D1 supply the binding site to P680 (PSII primary electron donor), Pheo (the first electron carrier intermediate), Q_B (a plastoquinone as the secondary electron acceptor), tyrosine (Tyr) and manganese (Mn)-cluster (involved in removing electrons from water). D2 supply the binding site to P680, Pheo, Q_A (a bound plastoquinone as the primary electron transfer) and Mn-cluster. All these redox components binding to D1 and D2 to form the first electron transfer chain.

The Chls of PSII RC participates in energy transfer from the proximal peripheral antennae complexes of CP43 (43-kDa, chloroplast *psb*C gene product) and CP47 (47-kDa, chloroplast *psb*B gene product) (Casazza et al., 2010). The antenna pigment-protein complex CP43-CP47 binds with RC and transfers excitation energy from the peripheral antenna of PSII (LHCII) toward the photochemical RC.

The water oxidation center (OEC) is associated with the PSII RC core, which has a Mn_4CaO_5 inorganic cluster ligated by waters and amino-acid side chains. The OEC is composed of three extrinsic polypeptides including OEE1 to 3 (Mayfield et al., 1987; Ohnishi and Takahashi, 2001; Alizadeh and Cohen, 2010). These three oxygen-

evolving enhancer proteins have different functions.

There are more than ten small (<10-kDa) hydrophobic peptides containing transmembrane helices, which are required for the assembly, stability or dimerization of the PSII complex. Some of the small polypeptides, such as PsbW (6-kD, nuclear gene *psb*W product) (García-Cerdán et al., 2011) is involved in PSII dimerization.

LHCII is involved in light energy transfer (Mozzo et al., 2008), photoprotection (Sunku et al., 2013), state transition between PSI and II (Minagawa, 2011), and grana thylakoids stacking (Wan et al., 2014). LHCII apoproteins of green algae and green plants which roughly corresponds to these proteins. They are classified mainly in two groups. One group including three subclasses named Lhcb1 (24.7~24.9-kD, 5 nucleus gene product), 2 (24.9-kD, 4 nucleus gene product) and 3 (24.3-kD, 1 nucleus gene product). These three apoproteins constitute LHCII trimer. Another group includes a small quantity of Lhcb4/CP29 (27.3~28.2-kD, 3 nucleus gene product), 5/ CP26 (26.1-kD, 1 nucleus gene product) and 6/CP24 (23.2-kD, 1 nucleus gene product).

LHCII is composited by about half of the Chl and one third of the protein of PS and associates PSII core complexes to form a large PSII-LHCII super complex (SC) with more than 1000-kDa molecular weight (Nelson and Junge, 2015).

1.2.2. PSI.

PSI complex consists of at around 19 protein subunits, approximately 100~200 Chl molecules, two phylloquinone and 3~4 Fe_4S_4 clusters (Fromme et al., 2001; Barros and Kühlbrandt, 2009). PSI RC is highly conserved among cyanobacteria, green algae, and green plants. In contrast, LHCI has lower conservation during evolution, possibly because of the difference of the strategy of environment adaption for the various light conditions (Pi et al., 2018).

PSI RC formed by PsaA-PsaB heterodimer as the heart that binds the vast major cofactors are supposed to consist of light harvesting cofactors, electron transfer cofactors, and terminal electron acceptors. Based on the different organism models,

light harvesting cofactors contain around 80~100 Chls *a* and around 20~30 β-carotenes. Electron transfer cofactors known as F_x contain 6 Chl *a* and 2 phylloquinone and a Fe_4S_4 cluster. Terminal electron acceptors are also known as Fe-S clusters F_A and F_B (Wientjes and Croce, 2011; Nickelsen and Rengstl, 2013). PSI RC accepts light-driven electrons from plastocyanin or cytochrome *c*6 on the lumenal side of the membrane and transfers to ferredoxin or flavodoxin at the stromal side through a chain of electron carriers, providing the reduction power for CO_2 fixing (Fromme et al., 2001).

Except for PsaA (~60-kD) and PsaB (~60-kD), the other subunits are a small size (4~18-kDa) with a different function: e.g. PsaC as ferredoxin docking at acceptor side; PsaK and PsaG as LHCI antenna system stabilization (Nelson and Ben-Shem, 2005; Barros and Kühlbrandt, 2009).

LHCI is known to be formed with four proteins called Lhca1–4 (20~24-kDa, 1 nuclear gene product each for Lhca1–Lhca4, and present in approximately equal amounts) (Storf et al., 2005), which binds to one side of the core complex where PsaG and PsaK locate (Jansson, 1994; Qin et al., 2015).

1.2.3. The Cyt $b_{559}f$ Complex.

The Cyt $b_{559}f$ complex is a central component of the photosynthetic electron transport chain of cyanobacteria, green algae and high plants (Kuras and Wollman, 1994). Cyt b_{559} including Cyt b_{559} α (9-kDa, chloroplast *psb*E gene product) and Cyt b_{559} β (4-kDa, chloroplast *psb*F gene product) (McNamara et al., 1997) function as haem binding, electron transfer from PSII to PSI component.

1.2.4. The ATPase enzymes Complex.

The ATPase enzymes also known as the F-ATPase, have been remarkably conserved in fungi, the chloroplast of green algae and land plants (Dekker and Boekema, 2005). This is a complex nanomotor that synthesizes nearly 90% of the ATP made during cellular respiration. F-ATPase consists of two coupled rotary motors: F_0-ATPase

complex, a mediates proton tunnel; and F_1-ATPase complex, the catalytic complex (Finazzi et al.; Leioatts and Grubmüller, 2015; Murakami et al., 2018).

1.3. Assembly of PSII.

PSII assembly is a sequential and highly coordinated process, exhibits a similar pathway found in cyanobacteria, green algae, and green plants. This suggests the core components of PSII and the assembly process of PSII complexes are conserved (Nixon et al., 2010; Nickelsen and Rengstl, 2013). PSII is assembled from smaller PSII modules via a series of distinct intermediates consist of a large -binding subunit, LMM membrane polypeptides, and associated pigments and other cofactors (Komenda et al., 2012).

1.3.1. Arabidopsis Model of PSII Assembly.

Firstly, Cyt $b_{559}f$ is assembled by PsbE and PsbF, accumulates in the thylakoid membrane as a central factor to initiate PSII assembly. D2 is assembled into Cyt $b_{559}f$ to form D2-Cyt $b_{559}f$ complexes. At the same time, precursor D1 (pD1) assembles with PsbI to form pD1-PsbI precomplexes. The next, two precomplexes form a sub-complex named PSII RC-like complex which locates in the membrane. The second step is CP47 binds into RC-like to form RC47a. LMM subunits including PsbH, T, M, and R binds with RC47a to form RCF47b. Meanwhile, LMM subunit PsbK with CP43 incorporates into RC47b to form the OEC-less PSII core monomer to finish the second step. The third step is the formation of PSII core monomer by assembly with OEC complexes and additional LMM subunits including PsbW and PsbZ.

The fourth step is the formation of LHCII. LHC apoproteins are partial insert into the inner chloroplast envelope via the chloroplast-vesicle-transport system located in developing thylakoids of young chloroplasts (Tanz et al., 2012; Khan et al., 2013; Karim and Aronsson, 2014). Then it is bound Chl located in the membrane. The rest of the protein domains are inserted with pigments binding into a fully assembled pigment-protein complex (Hoober et al., 2007; Dall'Osto et al., 2015) who locate at the inner chloroplast envelope. The final step is the dimerization of PSII core

complex, and assembly with LCHII to form the PSII-LHCII SC (Swiatek et al., 2003; Rokka et al., 2005; Torabi et al., 2014).

Even the PSII assembly procedure is highly conserved from cyanobacteria to green plants, the initial assembly steps of photosynthetic complexes appear to be spatially separated from sites of active photosynthesis (Lu, 2016). For example, in higher plants, it could be detected in the non-appressed stromal lamellae (Danielsson et al., 2006). In Chlamydomonas, the initial assembly occurs in discrete regions near the pyrenoid, called translation zones (Uniacke and Zerges, 2007).

1.3.2. Assembly Cofactors.

More than 60 auxiliary proteins, enzymes, or components of thylakoid protein trafficking/targeting systems are involved in the assembly, and/or the repair and reassembly cycle of PSII (Myouga et al., 2018; Yu et al., 2018). Such as PsbP-like proteins, atypical short-chain dehydrogenase/reductase family proteins and tetratricopeptide repeat proteins. A series of enzymes were discovered to catalyze important enzymatic steps, such as C-terminal processing of D1 (Nixon et al., 2010), thiol/disulfide-modulation (Ikegami et al., 2007), phosphorylation/dephosphorylation (Fristedt and Vener, 2011), and disassembly/repair (Järvi et al., 2015) of PSII proteins. These protein are absent in the crystallized complex (Komenda et al., 2012b). In these auxiliary proteins, some of them play a conserved role in cyanobacteria, algae, and plants, but some of them are specific and emerged after the evolution of the chloroplast (Mulo et al., 2008).

1.4. Photodamage and *de novo* Assembly of PSII.

For photosynthetic organisms, the excess light energy absorbed concomitantly damages the photosynthetic apparatus called photoinhibition or/and photodamage (Kato et al., 2012). To dissipate the excess energy and avoid photoinhibition, photosynthetic apparatus has developed a series of mechanisms that restrict the extent of photooxidative damage and that repair the damaged protein components. Because of PSII is more sensitive to light than other photosynthetic complexes, and the

photoinhibition is accompanied by oxidative damage to D1 that necessitates repair (Hatano-Iwasaki et al., 2000). A remarkable repair mechanism is evolved rather than the degrading and resynthesizing whole PSII. In this repair process, D1 protein with a dozen proteins, pigments, and cofactors are removed and replaced by the new synthesized (Mellis, 1999). This PSII repair cycle is an essential process to recover the PSII activity of oxygenic photosynthesis organisms (Ohad et al., 1984). Photoinhibition would occur when the repair rate is lower than PSII inactivation and photodamage rate (Dewez et al., 2009).

For *de novo* PSII assembly, PSII subunit synthesis is detected in discrete regions named for translation zones. While the repair of photodamaged PSII complexes occurs in the stroma lamellae of the chloroplast (Uniacke and Zerges, 2007). The first step of PSII reparation is the disassemble and migration of the damaged PSII RC from grana to stromal lamellae after disassembly of the PSII-SCs (Theis and Schroda, 2016). Secondly, the PSII core monomer would be migrated to stroma-exposed thylakoid membranes and dephosphorylated for D1 degradation (Lu, 2016). Thirdly, damaged D1 protein was replaced with the newly synthesized one inserting into CP43-free PSII monomers by *de novo* synthesis. The next step is followed with *de novo* step by re-assembly with OEC and then the PSII core monomer migrates back to grana stacks. Finally, the PSII monomer will be dimerized and reformed to be the PSII-LHCII super complex (Mulo et al., 2008; Järvi et al., 2015).

1.5. Degradation of PS System.

1.5.1. Several reasons for PSs Degradation.

Even though the involved factors of PSII repair mechanism show species specificity (e.g. Arabidopsis: low PSII accumulation 1 (LPA1) protein (Peng, 2006), Chlamydomonas: repair-aberrant 27 (REP27)) (Park et al., 2007a), it is highly conserved in all oxygenic photosynthesis organisms. Selective degradation of PS subunits protein is proceeded to remove the damaged protein by FtsH protease (Nixon et al., 2010; Malnoe et al., 2014; Wang et al., 2017). At this moment, the bound Chl *a* and Pheo *a* undergo concomitant turnover (Mullet et al., 1990; Beisel et al., 2010; Lin

et al., 2016).

Moreover, PS multi-subunit complexes could be assembled inefficiently because of the defects in a single subunit (e.g. *psb*D mutant), or in some complex. This kind of defection could lead to the degradation of all the subunits of the complexes (Henderson et al., 2003).

Green plants at the senescence stage or green algae in nutrient deficiency conditions (Schulz-Raffelt et al., 2016) would start the protein-pigment complex degradation procedure to recover nitrogen (N) and Carbon (C). In this situation, LHCII degradation is a crucial process for the acclimation to high light conditions (Yang et al., 1998) and for the recovery of nutrient during senescence (Guiamét et al., 2002).

1.5.2. Senescence.

Senescence is a responsive regulation to abiotic and biotic stress for plants (Wingler and Roitsch, 2008). Furthermore, natural senescence is an important process at the last stage of leaf development. It is characterized by dramatic changes in cellular metabolism and cellular structures. The earliest and most significant change in cell structure is the breakdown of chloroplast that contains up to 70% of the protein in leaves tissue (Ishida et al., 2008). The most obvious phenomenon is leaf colors changing from green to yellow or red (Zhou et al., 2011) caused by Chl degradation to recapture and delocalize nutrient (Lim et al., 2007). Chl degradation is a symptom of the transition of chloroplasts to gerontoplasts, which is the nucleus and chloroplast coordinated procedure to regulate senescence (Kusaba et al., 2013).

Senescence is regulated by a variety of external and internal factors. The external factors including the oxidation caused by UV-B (John et al., 2001; Sztatelman et al., 2015) and ozone (Miller et al., 1999). The harsh environment is one of the common external factors, including high/low temperature (Masclaux-Daubresse et al., 2006; Rossi et al., 2017), over/less light (Fukao et al., 2012; Zhu et al., 2017), drought and nutrient limitation. Notably, the programmed cell death caused by pathogen infection could overlap with senescence programs (Barth, 2004; Hörtensteiner et al., 2011).

The internal factors are reproduction and plant hormones such as ethylene (C_2H_4), cytokinin (CK)s, salicylic acid (SA), jasmonic acid (JA) and so on (Sembdner and Parthier, 1993; Version, 2008; Zhang et al., 2013; Hu et al., 2017). Plant hormones are divided into two groups, one group is the hormones which could promote senescence such as ethylene (Iqbal et al., 2017). And another group is the hormones which could inhibit senescence such as CKs (Gan and Amasino, 1995). Lack of plant hormones and its regulated genes could cause delayed senescence including proteolysis, Chl degradation, and C-N relocation.

1.5.3. Chl Degradation Pathway.

Chl degradation is tightly associated with the dismantling of pigment-protein complexes and the degradation of Chl-binding proteins (Lin et al., 2016). During senescence, Chl converts to colorless linear tetrapyrroles named nonfluorescent Chl catabolites (NCCs) as the final products of Chl degradation (Hörtensteiner, 2006). Degradation of Chl involves numerous and well-characterized steps and involves plastid and non-plastid reactions.

In this thesis, the green plants and green algae which contain Chl *a* and *b* would be discussed about their Chl degradation pathway. Because of Chl, *a* is the degradable form of Chls (Fig. 1), the first step for Chl *b* degradation is converting it to Chl *a* by two steps. Firstly, Chl *a* is converted to 7-hydroxymethyl Chl *a* (HMChl) *a* by Chl *b*

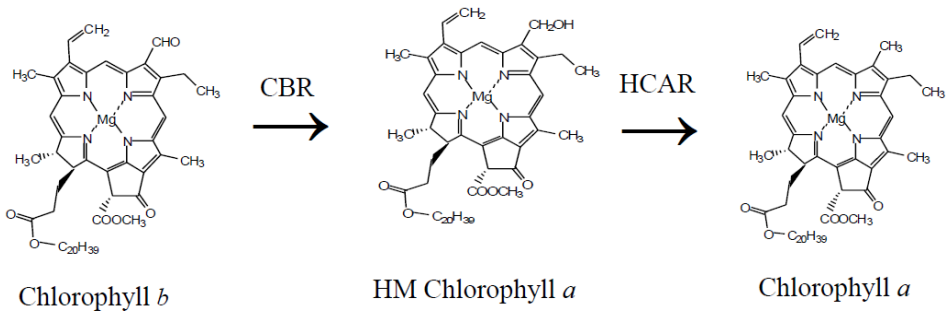

Fig. 1. The Pathway of Chl *b* Degradation. The first step of Chl degradation is conversion of Chl *b* to Chl *a*.

reductase (CBR) which are encoded by *NON-YELLOW COLORING* 1 (*NYC1*) and

NYC1-LIKE (*NOL*)) (Shimoda et al., 2012). Secondly, HMChl *a* is converted to Chl *a* by HMChl *a* reductase (HCAR) which is encoded by *HCAR*.

Then Chl *a* degradation (Fig. 2) will be continued catalyzed by Mg-dechelatase. This

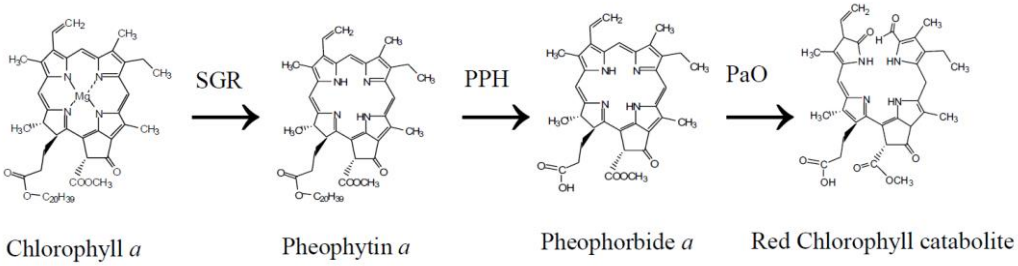

Fig. 2. A part of the Chl degradation pathway. Mg-dechelatase catalyzes the conversion of Chl *a* to Pheo *a*.

is encoded by *NON-YELLOWING*s/*STAY-GREEN*s (*NYE*s/*SGR*s) (Armstead et al., 2007a; Ren et al., 2007; Chen et al., 2016). Mg is initially removed from the central of Chl *a* to create Pheo *a*. Pheo *a* is hydrolyzed by PPH to produce pheophorbide (Pheide) *a*. Notably, Chl catabolites lose green color when the porphyrin ring of Pheide *a* is cleaved by PaO, resulting in oxidized red Chl catabolite (RCC) (Zhou et al., 2011).

RCC is turned to primary fluorescent Chl catabolite (pFCC) (Fig. 3) catalyzed by red Chl catabolite reductase (RCCR) (Thomas et al., 2002). Then pFCC is modified and transported into the vacuole, and isomerized to NCCs (Pruzinska et al., 2003).

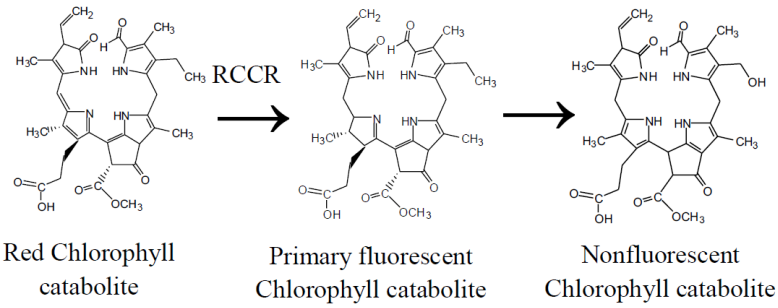

Fig. 3. The last stage of Chl degradation pathway in higher plants. The pathway of the late stage includes the cleavage reaction and steps after the reaction. And the products in late stage are colorless.

The Chl degradation pathway is highly conserved in high plants but still not fully elucidated in green algae and cyanobacteria (Hörtensteiner et al., 2011). While, in some mutants such as *NYC* (Sato et al., 2018), *PAO* (Thomas et al., 2002), *PPH* (Schelbert et al., 2009), SGR (Rong et al., 2013), the Chl degradation pathway is blocked to show a stay-green phenotype (Jibran et al., 2015) called as stay green mutants (Park et al., 2007b; Ren et al., 2007; Hörtensteiner et al., 2011; Shimoda et al., 2016).

1.6. The Stay Green Trait.

Stay green phenotype reflects impaired or delayed Chl catabolism, which means the mutants retain more Chls and photosynthetic capacity, which can be linked to higher yield (Jordan et al., 2012) and higher resistance (Borrell et al., 2014). It is well studied in several cereal crop species, such as wheat (*Triticum aestivum L*) (Luo et al., 2013a; Singh and Vaishali, 2016) and sorghum (*Sorghum bicolor* (*L.*) *Moench*) (Xu et al., 2000). Stay-green was divided into two groups, cosmetic stay-green and functional stay-green (Thomas and Howarth, 2000; Lim and Paek, 2015). In cosmetic stay-greens, all components of senescence syndrome are unaffected. The plant only shows maintained green color of leaves, because the primary lesion is confined to pigment catabolism (Morita et al., 2009). However, in functional stay-greens, the grain yield was increased through the sustained photosynthetic competence during monocarpic senescence in cereal crops (Fu et al., 2000; Zhou et al., 2011), and the entire senescence syndrome is delayed.

Stay-green genes encode members of chloroplast-located proteins (Thomas and Ougham, 2014), which are possibly functional to disable the Chl-apoprotein complexes in PSs or have the catalytic characteristics (Yoo et al., 2007; Matsuda et al., 2016). Meanwhile, the absence of a gene that controls the Chl degradation pathway also could cause the same stay-green phenotype even because of the different regulatory mechanism. Stay-green mutants exist in a mass of plant species (Hörtensteiner, 2009) and some of the stay-green genes are highly homologous.

1.7. *SGR*.

Mendel's green cotyledon gene is named *stay-green* (*SGR*). Its mutants are reported to be the visible stay green phenotype by Chl retention (Park et al., 2007b; Alos et al., 2008) in many species, such like Arabidopsis (*Arabidopsis thaliana*) (Shimoda et al., 2016), tomato (*Solanum lycopersicum*) (Luo et al., 2013b), rice (*Oryza sativa*) (Sato et al., 2007), pea (*Pisum sativum*) (Bell et al., 2015) and Alfalfa (*Medicago sativa*) (Zhou et al., 2011). In others species, it is named *SGR* (Jiang et al., 2007), *NONYELLOWING* (*NYE1*) (Ren et al., 2007), *GREEN-FLESH* (*GF*) (Cheung et al., 1993; Barry and Pandey, 2009), or *CHLOROPHYLL RETAINER* (*CL*) (Barry et al., 2008).

Green plant Arabidopsis have three *SGR* genes, *SGR1*, *SGR2,* and *SGRL*, but green algae Chlamydomonas only have one *SGR* (Yasuhito et al., 2015). The Arabidopsis *sgr1* and *sgr2* showed gradually increasing expression level during the development of plants, suggesting that *SGR1* and *SGR2* might be involved in senescence regulation by Chl degradation (Barry et al., 2008; Delmas et al., 2013; Wu et al., 2016; Li et al., 2017). Meanwhile, the Arabidopsis *sgrl* show the adverse expression pattern, suggesting it might be involved in stressful environment response (Sakuraba et al., 2014) or Chl degradation like in pea (Bell et al., 2015) and rice (Rong et al., 2013). The function of Chlamydomonas SGR is identified as an Mg-dechelatase in vitro experiment (Matsuda et al., 2016) like Arabidopsis SGR (Shimoda et al., 2016). But the physiological function of Chlamydomonas *SGR* is not investigated yet.

1.8. The strategy of Pheo *a* supply.

Arabidopsis and Chlamydomonas SGR convert Chl *a* to Pheo *a* by removing Mg from the center of Chl *a* (Matsuda et al., 2016; Shimoda et al., 2016). The formed Pheo *a* would proceed to the next degradation step to finish Chl degradation observed in senescence stage and disassemble/repair procedure.

The Chl composition of D1/D2 heterodimer complex is different from that of other LHC because only the RC complex contains Pheo *a* in addition to Chl *a*, suggesting

that supply Pheo *a* may contribute in RC complex formation. However, the impact of Pheo *a* synthesis on the formation of PSII has never been addressed before. Because the production mechanism of Pheo *a* has been unknown for a long time (Hörtensteiner, 2012; Shimoda et al., 2016). The Mg in Chl is spontaneously released under acidic conditions (Saga et al., 2013), which led to the hypothesis that Pheo *a* is nonenzymatically produced from Chl *a* under such conditions (Christ and Hörtensteiner, 2014).

SGR could catalyze the convert from Chl *a* to Pheo *a* by removing Mg. These studies clearly show that Pheo *a* is not only spontaneously produced but also enzymatically synthesized. There are three hypotheses now for the production of Pheo *a* in PSII formation: Firstly, Pheo *a* is produced by SGR. Secondly, Pheo *a* is produced by an unidentified Mg-dechelatase. Thirdly, Pheo *a* is formed in the PSII RC.

Because of Chlamydomonas could grow heterotrophically without PSII, Chlamydomonas *sgr* mutants which have low PSII core but unchanged PSI and LHCII levels were used. These phenotypes were different from Arabidopsis *sgr* triple mutants which have the unaffected PSs levels compared with wild type (WT). Based on these results, we discussed the role of *SGR* in the formation and degradation of PSs from an evolutionary viewpoint.

2. Materials and Methods

2.1. Organisms Sources.

Arabidopsis (Columbia ecotype) wild type (WT) used in this study, *sgr* triple mutants were obtained by crossing mutants lacking *SGR1* (Ren et al., 2007), *SGR2* (SALK_003830C) and *SGRL* (SALK_084849). Genomic DNA PCR was used to confirm the mutation. The *sgr2* and *sgrl* mutants were obtained from the Arabidopsis Biological Resource Center.

Chlamydomonas WT (CC-1618 cw15 arg7 mt-) were used for this study, PsbD deletion mutants were purchased from the Chlamydomonas Resource Center.

2.2. Culture and Growth Conditions.

Arabidopsis plants were grown on soil under long day (16 h light equipped with white fluorescent lamps at the light intensity around 90 μmol photons m^{-2} s^{-1} (NL90): 8 h dark) conditions at 22 ℃ (Shimoda et al., 2016).

Suspension cultures of Chlamydomonas were grown in TAP medium photomixotrophically or in HSM medium (HSM medium growth curve only) photoautotrophically. Mutation screening cultures of Chlamydomonas were grown in TAP solid medium with antibiotics. Forty mL Erlenmeyer flasks culture were shaken at 120 rpm under continuous fluorescent light (1 μmol photons m^{-2} s^{-1}, LL1; 80 μmol photons m^{-2} s^{-1}, NL80 (in all the experiments excepted more descriptive information); or 250 μmol photons m^{-2} s^{-1}, HL250) at 25 °C.

2.3. Dark Treatment for Senescence Introduction.

Arabidopsis detached leaves were transferred to a whole set of 24 well tissue culture plates with water surrounded at the outermost side of the plate. The plates were sealed and covered with aluminum foil and placed in the paper box. The detached leaves were put at the same growth conditions without light.

2.4. Strong Light Treatment for Arabidopsis and Chlamydomonas.

Chlamydomonas logarithmic phase cells grown at NL80 were used for these experiments. To avoid the interference caused by thermal damage, the Chlamydomonas culture flasks were physically insulated from shaker by a thermal baffle. Chlamydomonas cultures were exposed to SL750 for 60 h strong light treatment and Fv/Fm ratios were measured each 12 h after 10 min of dark adaption.

2.5. Construction of Mutant Library of Chlamydomonas.

The pSI-103 vector obtained from Chlamydomonas Resource Center was used to generate the mutant library by DNA insertional mutagenesis (Tanaka et al., 1998). The strategy for isolating Chlamydomonas *sgr* mutants is the hypothesis of the relation between photosystem activity and the function of *SGR*, details are described in Results. For the identification of a DNA region flanked by the inserted T-DNA, TAIL (thermal asymmetric interlaced)-PCR was carried out (Matsuo et al., 2008).

2.6 Complementation of Chlamydomonas *sgr* Mutants.

Chlamydomonas SGR cDNA was prepared by PCR, and specific primers of SGR (*Cr_SGR*) were listed in Table. 1. Amplified fragments were introduced into the pChlamy_1 vector (Invitrogen) between the *Nco*I and *Not*I sites. The *Nco*I site was created by modifying the original start codon. Fv/Fm ratios of Chlamydomonas grown on the agar plates were measured using FluorCam 701MF to select the complemented cell, and then confirmed by genomic PCR.

Table. 1 Primer list of PCR for preparation and confirmation of Chlamydomonas complimented lines.

Name	Primer sequence (5' to 3')
Cr_SGR-F	CACTCAACATCTTACGGTAAGTATGTTAGACACGACTTGG
Cr_SGR-R	TCATATGGCGGCCGCCAACAGGTCATGTTACAGGGGGCAT

2.7. Complementation of Arabidopsis *sgr* Triple Mutants.

CrSGR with the Arabidopsis SGR1 transit peptide was prepared as previously described (Matsuda et al., 2016). This fragment was introduced into the Gateway entry vector pENTR4 Dual and then introduced into the Gateway-compatible inducible vector pEarleyGate 100. The construct was transferred into Agrobacterium tumefaciens (strain GV3101) and transformed into the Arabidopsis *sgr* triple mutant using a floral dip method. Transgene expression was driven using the 35S promoter and Arabidopsis SGR1 (2 kbp) promoter which amplified from Arabidopsis genomic DNA using specific primer sets *AtSGR1_promoter* listed in Table. 3 and fused with the Chlamydomonas SGR with the Arabidopsis SGR1 transit peptide. This construct was introduced into Arabidopsis using pEarleyGate301 and confirmed by genomic DNA PCR using the specific primers sets *CrSGR_T* to amplify CrSGR using the terminator fragments listed in Table. 2.

Table. 2 Primer list of PCR for preparation and confirmation of Arabidopsis complimented lines.

Name	Primer sequence (5' to 3')
AtSGR1_promoter-F	GCAGGCTCCACCATGGATTGCAGGATGTTATAAG
AtSGR1_promoter-R	AACTACACATCTCTGCTTGAAACCCA
AtSGR_CrSGR-F	GAGAGCAGAGATGTGTAGTTTGTCGGCGAT
CrSGR_pENT-R	AAGCTGGGTCTAGATTCACTTGTCGTCATCGTCTT
AtTransit_pENT-F	GCAGGCTCCACCATGTGTAGTTTGTCGGCGATTAT
CrSGR_T-F	TGAGGAGGACCAGCAGCAAC
CrSGR_T-R	GAACCGAAACCGGCGGTAAG
ACT2-F	AGTGTTGTTGGTAGGCCAAG
ACT2-R	CAGTAAGGTCACGTCCAGCA
CrSGR-F	GGCACAAGTAGCAGCAGTAG
CrSGR-R	CACTTGTCGTCATCGTCTTTG

2.8. Measurement of Fv/Fm Ratios.

Fv/Fm ratios were measured using FluorCam 701MF and PAM-2500 (Walz) chlorophyll (Chl) fluorometer after 10 min of dark acclimation.

2.9. Pigment Extraction and High-Performance Liquid Chromatography (HPLC) Analysis.

Arabidopsis plants leaves were ground by the liquid nitrogen cooled grinder and resuspended by 20 times fresh weight acetone. Chlamydomonas cells were harvested by centrifugation at 22,500 × g for 1 min and resuspended in 50 μL water, then adding 200 μL acetone for pigment extraction. These solutions were mixed vigorously for 1 min and centrifuged at 22,500 × g for 10 min.

Twenty μL supernatant was subjected, RF20A fluorescence detector and a SPD-M10A diode array detector (Shimadzu), symmetry C8 column (150 mm in length and 4.6 mm in inner diameter; Waters), were used for the HPLC system (Shimoda et al., 2016). Calibration curves of known pigments were constructed to quantify Chl and pheophytin (Pheo). Violaxanthin (Viol) and neoxanthin (Neo) was relatively quantified by leaves area.

2.10. Blue Native Polyacrylamide Gel Electrophoresis (BN-PAGE) Analysis.

Arabidopsis leaves were ground with liquid nitrogen cooled grinder and resuspended by two times fresh weight cooled buffer (named BN-solubilization buffer in this thesis) containing 50 mM imidazole/HCl (pH 7.0), 20% (wt/vol) glycerol, 5 mM 6-aminocaproic acid, 1 mM EDTA and 1% (vol/vol) Protease inhibitor cocktail (Sigma).

Chlamydomonas logarithmic phase cells were harvested by centrifugation at 7,000 × g for 5 min at 4 °C, then resuspended in cooled BN-solubilization buffer. Cells were disrupted using a Mini-bead beater with 0.5 mm diameter glass beads at 5,000 rpm for 60 s, each 20 s as an interval on ice.

These homogenates were centrifuged at 22,500 × g for 1 min at 4 °C. The pellet was washed twice with cooled BN-solubilization buffer, then resuspended and mixed with

the same volume of 2% (wt/vol) α-dodecyl maltoside (α-DM), the final Chl concentration would reach 0.25~0.5 μg/μL. The 10 μL Arabidopsis and Chlamydomonas supernatant containing membrane proteins were separated on a 4~14% acrylamide gradient gel at 4 °C (Takabayashi et al., 2011).

2.11. Second Dimensional (2D) Electrophoresis.

Following electrophoresis, bands from Chlamydomonas BN-PAGE gel were excised to gel pieces. An electrophoresis lane gel from Arabidopsis and the gel pieces from Chlamydomonas were heated at 80 °C for 3 min in 100 μL water and cooled to room temperature. The same volume buffer (named solubilizing buffer in this thesis) containing 10% (wt/vol) sucrose, 125 mM Tris-HCl (pH 6.8), 4% (wt/vol) SDS, 1% (wt/vol) bromophenol blue and 10% (vol/vol) 2-mercaptoethanol was added to the heated sample and equilibrated for 5 min. Sodium dodecyl sulphate polyacrylamide gel electrophoresis (SDS-PAGE) with 14% separation gel and containing 8 M urea were performed as reported previously (Takabayashi et al., 2011).

2.12. Silver Staining.

After running the gel in electrophoresis apparatus, BN-2D/SDS-PAGE gel was incubated by fixative solution A containing 50% (vol/vol) methanol and 10% (vol/vol) acidic acid for one hour with gentle shaking. Secondly, transfer gel to fixative solution B containing 20% (vol/vol) methanol, 7% (vol/vol) acidic acid and 0.05% (wt/vol) thiourea for 15 min. Next step is transfer gel to pretreatment solution containing 47% (vol/vol) methanol, 0.26% (vol/vol) Gultaraldehyde and 1.05% (wt/vol) DTT for 10 min. The gel was washed 3 min by Milli-Q water for twice then stained by staining solution containing 1% (wt/vol) $AgNO_3$, 1% (vol/vol) ammonia solution, 2.5% (wt/vol) NaOH for 8 min. The gel was washed 3 min by MQ water for three times and then developed with developing solution containing 0.05% (vol/vol) formaldehyde, 0.005% (wt/vol) citric acid for 3 min (Takabayashi et al., 2011).

2.13. Low-Temperature Fluorescence Analysis of BN-PAGE gel.

Green bands of BN-PAGE gel (for Chlamydomonas only) were put into glass tubes and frozen in liquid nitrogen immediately. Low-temperature emission spectra were measured by exciting frozen samples at 440 nm, an F-2500 fluorescence spectrophotometer (Hitachi) was used to perform this experiment.

2.14. Sodium Dodecyl Sulfate Polyacrylamide Gel Electrophoresis (SDS-PAGE) Analysis.

Arabidopsis 2-week-old plant leaves were homogenized with 20 times (wt/vol) solubilizing buffer. Chlamydomonas logarithmic phase cells were harvested by centrifugation at 7,000 × g for 5 min at 4 °C, then resuspended in solubilizing buffer. The homogenate was centrifuged at 22,500 × g for 1 min at room temperature, and 1 μL of supernatant was resolved with 14% polyacrylamide gel perform SDS-PAGE Analysis.

2.15. Immunoblotting Analysis.

SDS-PAGE was performed, and the components were electroblotted to PVDF membrane. Primary antibodies against CP43 (1:10,000) (Tanaka et al., 1991), CP47 (1:10,000, Agrisera), D1 (1:10,000, Agrisera), D2 (1:10,000, Agrisera), LHCII (1:5,000) (Tanaka et al., 1991), PsaA (1:2,000, Agrisera) and PsaC (1:10,000, Agrisera), PsaA/PsaB (1:100,000) (Tanaka et al., 1991); and appropriate secondary antibodies (1:10,000, Sigma) were used.

2.16. Low-Temperature Fluorescence Analysis of Chlamydomonas Cells.

Chlamydomonas logarithmic phase cells were adjusted to 0.5 μg Chl/mL in the dark environment, then immediately frozen in liquid nitrogen with 25% (vol/vol) glycerol. Low-temperature emission spectra were measured by exciting frozen samples at 440 nm using F-2500 fluorescence spectrophotometer (Hitachi).

2.17. P700/Chl Measurement of Chlamydomonas.

Chlamydomonas logarithmic phase cells were centrifugation at 7,000 × g for 5 min at 4 °C and resuspended in buffer containing 25mM Tricine-NaOH (pH 8.0), and 0.1% Nonidet P-40 by adjusting the Chl content at 20μg/mL. P700/Chl was measured by previous reports (Tanaka et al., 1991).

2.18. Nitrogen (N) Starvation Treatment.

Chlamydomonas logarithmic phase cells cultured in TAP medium were harvested by low-speed centrifugation and resuspended in TAP-N- medium (Sharma et al., 2015) and TP-N-medium with constant air flow containing 5% CO_2, respectively.

2.19. RNA Extraction and Real-Time Polymerase Chain Reaction (qRT-PCR).

From Chlamydomonas cells, 4- and 9-week-old Arabidopsis leaves total RNA was extracted using an RNeasy mini kit (Qiagen), cDNA was synthesized by PrimeScriptRT reagent kit with gDNA Eraser (TaKaRa), and qRT-PCR was performed by an iQ5 Real-time detection system (Bio-Rad). Primer pairs for Chlamydomonas are listed in Table. 3 and Chlamydomonas G protein β-subunit-like polypeptide (CBLP) was used as a control. Data were analyzed with iQ5 Optical system software (Bio-Rad).

Table. 3 Primer list of qRT-PCR for nitrogen starvation of Chlamydomonas.

Name	Primer sequence (5’ to 3’)
NYC1-F	CGGGTGGAGGACACATCTTC
NYC1-R	TGACTGTGTGCAGCTTGATG
PaO-F	CAAGCTCATCTCGAACATCC
PaO-R	GCCACTCATCTCGAACATCC
SGR-F	TTCATTTCCAGTCCAGCGTG

SGR-R	CGATGATGGCGTAAATGGTG
CBLP-F	GATGTGCTGTCCGTGGCTTTC
CBLP-R	ACGATGATGGGGTTGGTGGTC

3. Results

3. 1. Chlamydomonas *sgr* Mutants Isolation.

The strategy of mutant isolation was based on the hypothesis that photosystem (PS) II formation depends on supplying of pheophytin (Pheo) *a*. Fv/Fm ratio gives a robust indicator of the maximum quantum efficiency of PSII (Murchie and Lawson, 2013). The mutant library was generated using insertional DNA mutagenesis in the first step. Mutagenized Chlamydomonas cells were grown on agar plates containing antibiotics for mutation screening. To avoid the photodamage, Chlamydomonas cells were cultured under low light conditions to carry out the first-round mutation screening. Using approximately 80,000 independent Chlamydomonas mutant colonies, Fv/Fm ratios were measured using a chlorophyll (Chl) fluorometer imaging system (FluorCam), and low Fv/Fm ratios colonies were selected with a highly variable size.

These colonies were cultured in liquid TAP medium for the second screening. Fv/Fm ratios were determined using a PAM Chl fluorometer to isolate 200 mutants with low Fv/Fm ratios which were below 0.5 (healthy wild type (WT) was around 0.8). Thermal asymmetric interlaced (TAIL)-PCR were performed with these 150 mutants which flanked by the inserted DNAs for the DNA regions. Assuming a large genomic DNA deletion of following the DNA insertion (Tanaka et al., 1998), these 150 mutants were classified into 60 groups, each with 1–7 independent mutants. One of these groups in which the *SGR* gene was deleted were confirmed by genomic PCR (Fig. 4). Two of Chlamydomonas null *sgr* mutants were obtained and used for further experimental analyses.

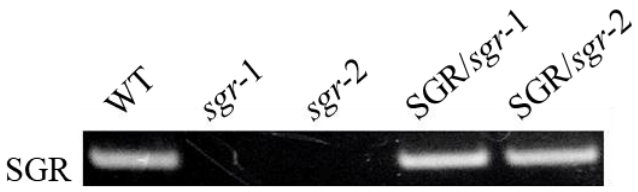

Fig. 4. Genomic PCR of confirmation Chlamydomonas null *sgr* mutants and *sgr* complementation. Chlamydomonas cells were grown in TAP medium at NL80.

3. 2. Fv/Fm Ratios Analysis under Several Light Intensity.

The effects of light intensity on the Fv/Fm ratio was preclusive. Under normal light conditions (80 μmol photons m^{-2} s^{-1}, NL80), the Chlamydomonas *sgr* mutants exhibited half levels (around 0.4) Fv/Fm ratios compared to WT (around 0.8) (Fig. 5). The intact Chlamydomonas *SGR* gene was introduced into genomes of the two Chlamydomonas *sgr* mutants to confirm that the mutant phenotypes were caused by *SGR* gene deletion, which was confirmed by the restored Fv/Fm ratios similar (around 0.8) to WT level in two complementation lines (Fig. 5). Fv/Fm ratios of the two Chlamydomonas *sgr* mutants and the two complementation lines under extremely low light conditions (1 μmol photon m^{-2} s^{-1}, LL1) (Fig. 5) were like those of NL80 indicating that the low Fv/Fm phenotypes were caused by *SGR* gene deletion but not by photodamage. Under high light conditions (250 μmol photons m^{-2} s^{-1}, HL250), the Fv/Fm ratios showed decreased levels in all lines including WT, two Chlamydomonas *sgr* mutants, and two complementation lines. Notably, the Fv/Fm ratios of the two Chlamydomonas *sgr* mutants were reduced under extremely low light conditions (LL1) (Fig. 5). All these results indicate that the low Fv/Fm ratios of the two Chlamydomonas *sgr* mutants are not caused by photoinhibition or photodamage.

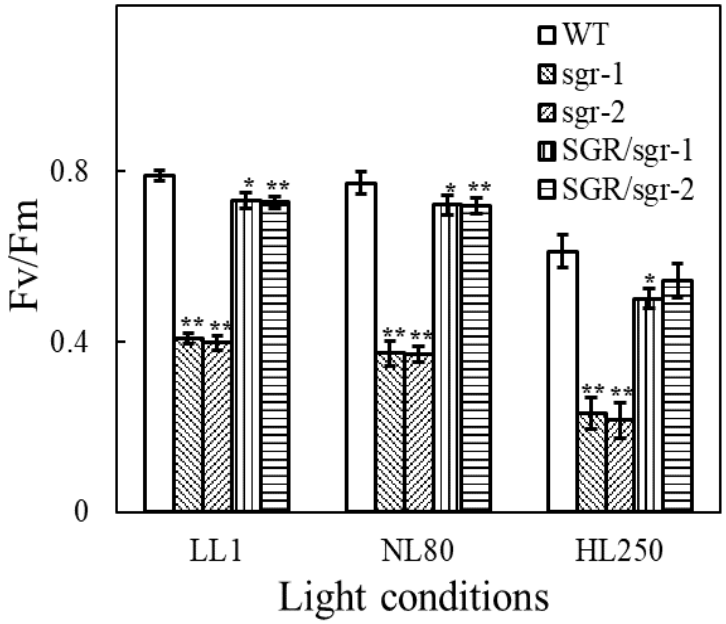

Fig. 5. The affection of light intensity on Fv/Fm ratios in Chlamydomonas cells. Chlamydomonas cells were cultured in TAP medium at NL80 to stationary growth phase, then exposed to LL1, NL80, or HL250 for 2 days. The Fv/Fm ratios were measured after 10 min of dark acclimation. Measurements from 3–6 biological replicates (mean ± SD) that were significantly different from WT are indicated (** $P < 0.01$, * $P < 0.05$, Student's t-test).

The previous reports showed that the reduced PSII levels are the result of the photosensitive phenotypes, which includes easily photodamaged and reduced recovery speed from photoinhibition. The second step is the examination to the strong light conditions (750 μmol photons m^{-2} s^{-1}, SL750) response of all Chlamydomonas materials which were grown under NL80 light to stationary phase and then exposed to SL750 conditions. The Fv/Fm ratios were reduced by strong light treatment and only remained about 0.2 in WT while rapidly reduced to 0 and did not recover in the two Chlamydomonas *sgr* mutants (Fig. 6). The unrecovered Fv/Fm ratio of Chlamydomonas *sgr* mutants might be because of the cell death caused by strong light treatment. This result showed a deficiency of *SGR* has a positive correlation with the increased photosensitivity and reduced photo recovery ability.

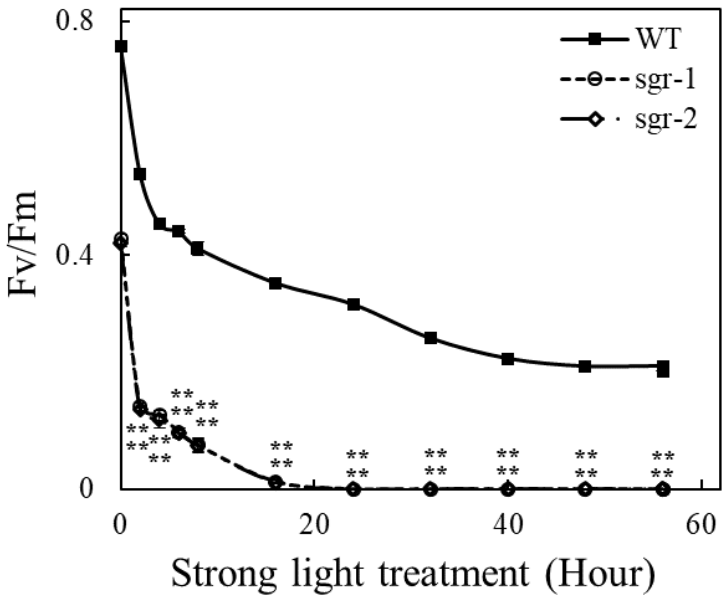

Fig. 6. The affection of photoinhibition on Fv/Fm ratios in Chlamydomonas cells. Chlamydomonas cells were cultured in TAP medium at NL80 to stationary growth phase, then exposed to SL750 for 60 hours. The Fv/Fm ratios were measured after 10 min of dark acclimation. Measurements from 3–6 biological replicates (mean ± SD) that were significantly different from WT are indicated (** $P < 0.01$, Student's t-test).

3. 3. Growth Rates Analysis at Photomixotrophically and Photoautotrophically Conditions.

The carbon source is necessary for Chlamydomonas. One of the functions of PSII is

to fix the carbon for plant survival. It is necessary to examine the photoautotrophic ability to further explanation whether the PSII is functional or not in the two Chlamydomonas *sgr* mutants. At the same time, photomixotrophic ability is necessary to illuminate deeper understanding of the function of Chlamydomonas *SGR* to PSII formation. The effects of carbon source TAP medium (Fig. 7), deficiency HSM medium (Fig. 8) to the growth rate of the *SGR* mutation were examined. The two Chlamydomonas *sgr* mutants showed reduced growth rates while the two complemented lines showed similar growth rates (Fig. 7) to the WT under NL conditions in either medium. The Chlamydomonas *sgr* mutants could grow photoautotrophically (Fig. 8) but showed reduced growth rates, indicating partly formation of functional PSII. These experiments showed that active PSII was partly formed in Chlamydomonas *sgr* mutants to support the photoautotrophic growth, and the *SGR* is involved in the active PSII formation in Chlamydomonas.

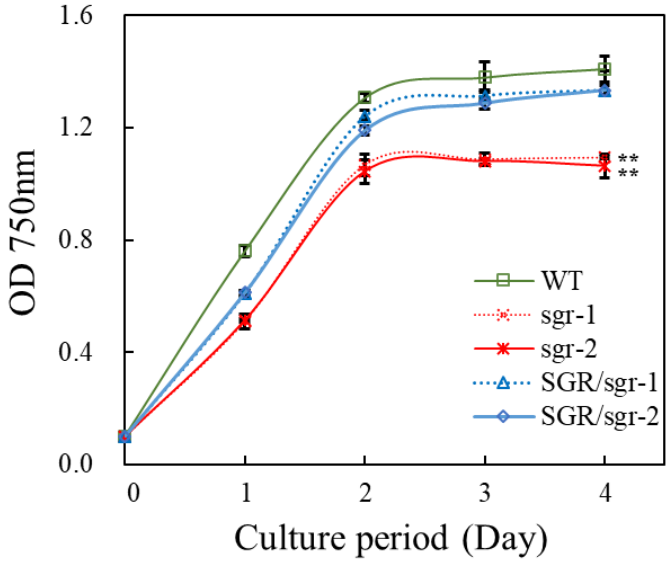

Fig. 7. Growth rates under photomixotrophic conditions. Chlamydomonas cells grown at NL80 were inoculated at an optical density of 0.1 at 750 nm and grown photomixotrophically. Measurements from 3–6 biological replicates (mean ± SD) that were significantly different from the WT are indicated (** $P < 0.01$, Student's t-test).

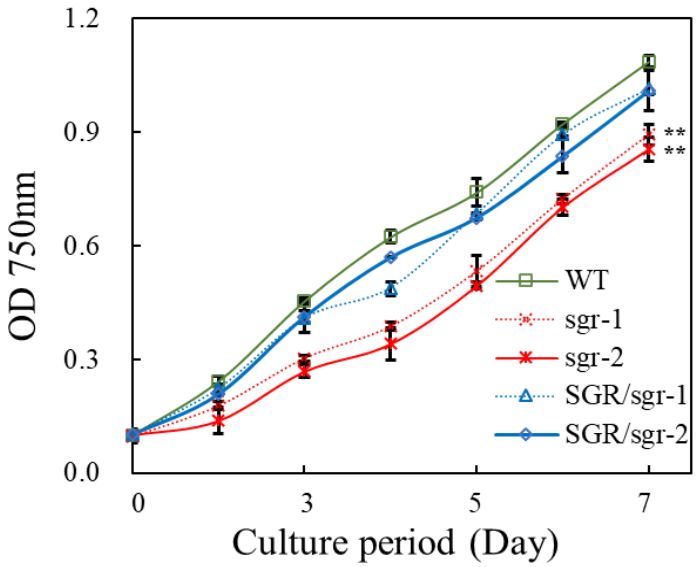

Fig. 8. Growth rates under photoautotrophic conditions. Chlamydomonas cells grown at NL80 were inoculated at an optical density of 0.1 at 750 nm and grown photoautotrophically on HSM medium. Measurements from 3–6 biological replicates (mean ± SD) that were significantly different from the WT are indicated (** $P < 0.01$, Student's t-test).

3. 4. Measurement of Pheo *a* Accumulation Levels.

The previous report showed that Chlamydomonas SGR catalyzes the degradation of Chl *a* to converting it to Pheo *a* (Matsuda et al., 2016). One of the possible reasons for the reduced Fv/Fm ratio is a limited supply of Pheo *a* for PSII formation which is caused by lack of *SGR*. The size of Pheo *a* pool was measured using high-performance liquid chromatography (HPLC). The Pheo *a*/Chl ratio level was around 0.009 in the WT (Fig. 9) at the very early growth phase where the optical density at 750 nm was around 0.1 (Fig. 7). This value is largely consistent with a previous report, which found a Chlamydomonas WT Chl/Pheo *a* ratio was 100 (Garnier et al., 1990).

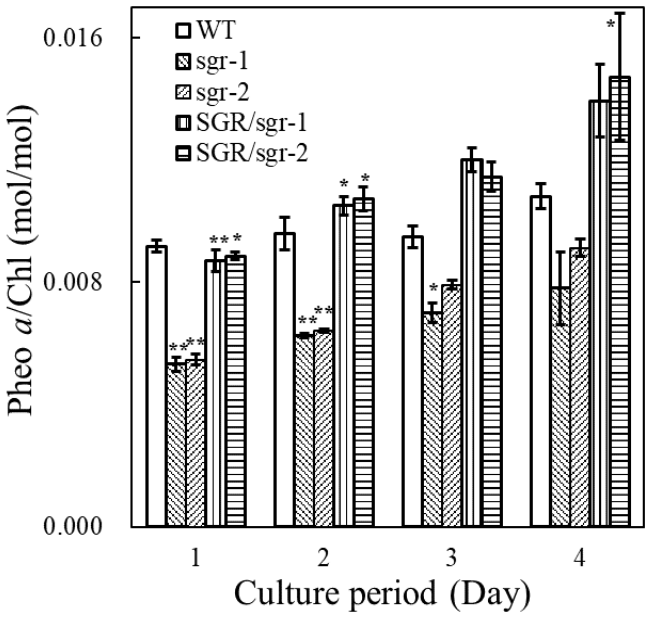

Fig. 9. The Pheo *a*/Chl ratios of *sgr* mutant and *sgr* complemented mutant during the growth phase. Chlamydomonas cells were grown in TAP medium at NL80 which inoculated at an optical density of 0.1 at 750 nm. Measurements from 3–6 biological replicates (mean ± SD) that were significantly different from the WT are indicated (** $P < 0.01$, * $P < 0.05$, Student's t-test).

The Pheo *a*/Chl ratios in the Chlamydomonas *sgr* mutants were around 60% of WT (Fig. 9) and similar to *psb*D mutant (Fig. 10) at the same growth phase. The introduction of the *SGR* gene into the Chlamydomonas *sgr* mutants increased Pheo *a*/Chl levels (Fig. 9) even beyond WT, in keeping the increased Fv/Fm ratios (Fig. 5). These results indicate that reduced photosystem activity and photosynthesis ability in two Chlamydomonas *sgr* mutants were caused by the restricted Pheo *a* supply. The Pheo *a* levels were increased accompanied with the culture time by unclear reasons. One of the possible reasons is partial Chl degradation or cell death during the later culture period.

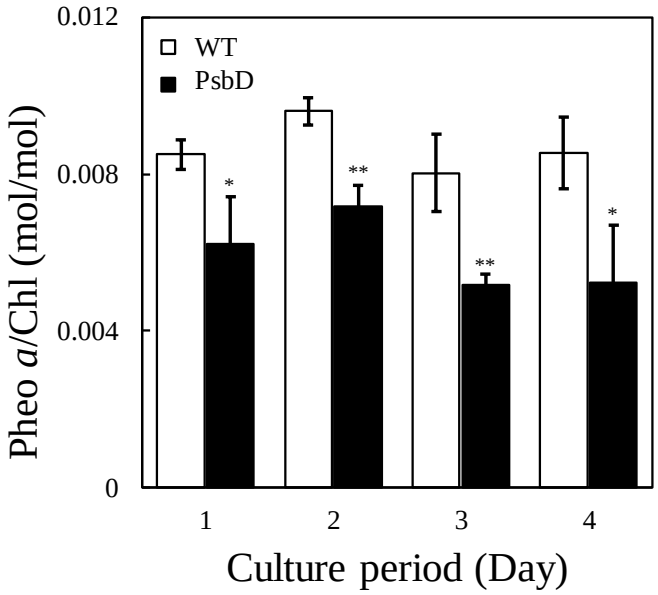

Fig. 10. The Pheo *a*/Chl ratios of *psb*D mutant during the growth phase. Pheo *a*/Chl ratios of the WT and *psb*D mutant during the growth phase. Chlamydomonas cells were grown in TAP media at NL80 and were inoculated at an optical density of 0.1 at 750 nm. Measurements from 3–6 biological replicates (mean ± SD) that were significantly different from the WT are indicated (** $P < 0.01$, * $P < 0.05$, Student's t-test).

3. 5. The Pigment Levels Analysis of Chlamydomonas *sgr* Mutants.

To further examine the pigment-proteins complexes change caused by the Chlamydomonas *SGR* defect, the Chl levels of Chlamydomonas WT and *sgr* mutants during the growth span were investigated using HPLC. The Chl levels of the two Chlamydomonas *sgr* mutants were 50% of the WT (Fig. 11) at the very early growth phase when the optical density at 750 nm around was 0.1 (Fig. 7). This Chl ratio (Chlamydomonas *sgr* mutant/WT) was not increased during the culture period. The introduction of the *SGR* gene into the *sgr* mutants recovered the Chl levels (Fig. 11) similar to WT. These results suggest that the defect of Chlamydomonas *SGR* could cause the pigment-protein complex partially formation.

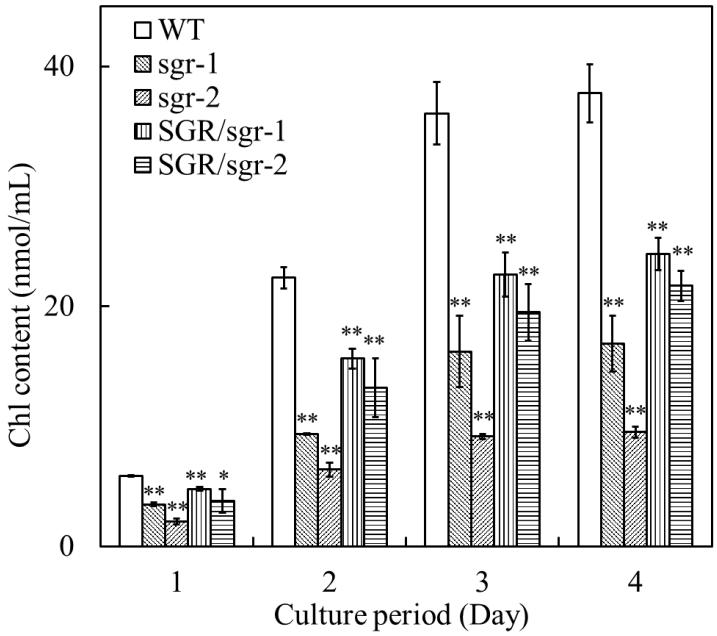

Fig. 11. The Chl levels during the growth phase. Chlamydomonas cells were grown in TAP media at NL80 and were inoculated at an optical density of 0.1 at 750 nm. Measurements from 3–6 biological replicates (mean ± SD) that were significantly different from the WT are indicated (** $P < 0.01$, * $P < 0.05$, Student's t-test).

3. 6. BN-PAGE Analysis of Chlamydomonas.

Pigment analysis (Fig. 9, Fig. 11) suggested that PSII formation was defective in the Chlamydomonas *sgr* mutants. To examine whether the PSs were properly formed, Chlamydomonas WT and the *sgr* mutants were cultured for BN-PAGE analysis to know the PSs levels (Fig. 12). Compared with WT, the Chlamydomonas *sgr* mutant showed reduced PSII-LHCII super complex levels shown in band 1, 2 and 3. In band 4, 5, 6 and 7, Chlamydomonas *sgr* mutants showed similar levels as WT. Band 4 and 5 of BN-PAGE gel, which might mainly be PSI-LHCI, band 6 and 7 should be LHCII trimer and monomer. The introduction of the *SGR* gene into the Chlamydomonas *sgr* mutants induced the PS levels (Fig. 12) even beyond WT, in keeping with the increased Fv/Fm ratios (Fig. 5). This result means Chlamydomonas *SGR* is functional to PSII proteins formation.

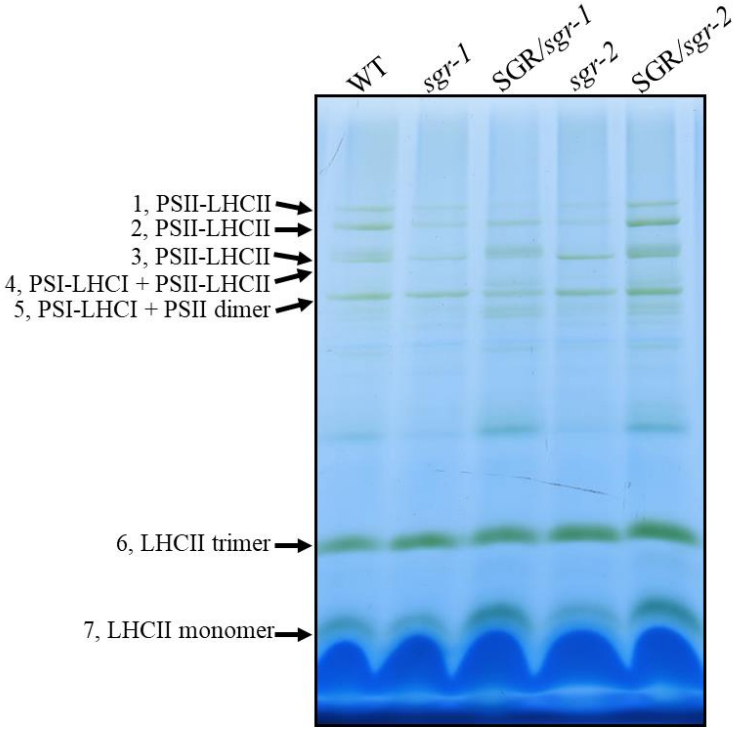

Fig. 12. BN-PAGE analysis of the photosystems of Chlamydomonas. Chlamydomonas cells were grown in TAP medium at NL80, and the photosystems were resolved using BN-PAGE.

3. 7. Low-Temperature Fluorescence of BN-PAGE Bands of Chlamydomonas.

To identify the components in each major green band from BN-PAGE analysis, the low-temperature fluorescence spectra of bands 1–5 (Fig. 13) were measured using Hitachi F-2500 Fluorescence Spectrophotometer and data were analyzed using Microsoft Excel. Even though Coomassie brilliant blue quenches the LHCII excitation energy (Yokono et al., 2015), PSI and PSII fluorescence signal from BN-PAGE gels still could be detected. In Chlamydomonas WT, bands 1, 2 and 3 exhibited similar fluorescence spectra, each with a peak of around 690 nm as the characteristic of a PSII spectrum. Band 4 exhibited mainly PSI fluorescence spectra with a small PSII peak and PSI-LHCI signals. Band 5 also exhibited fluorescence peaks of both PSs, it contained PSI-LHCI and the PSII-dimer, which are already known by co-migrate (Takabayashi et al., 2011). The intensities of bands 1, 2 and 3 from Chlamydomonas *sgr* mutants (presented *sgr*-1 mutant only, *sgr*-2 mutant showed similar results and data not shown) were reduced compared with those of WT.

Fluorescence at approximately 720 nm in these three bands of Chlamydomonas *sgr* mutants could be derived from contaminated PSI. The PSII fluorescence was dominant in band 4 of Chlamydomonas *sgr* mutant which is slightly different from the WT which showed the higher PSII and lower PSI signals. Band 5 of Chlamydomonas *sgr* mutant had a fluorescent peak at around 720 nm of PSI and a very low or lack of peak corresponding to PSII. The intensities of the PSI (bands 4 and 5) and LHCII bands (bands 6 and 7) were not particularly different between Chlamydomonas WT and *sgr* mutants. These results implied that the PSII and its components were affected but PSI and LHCII were not affected by Chlamydomonas *SGR* deletion, that is consistent with the HPLC and BN-PAGE analysis results.

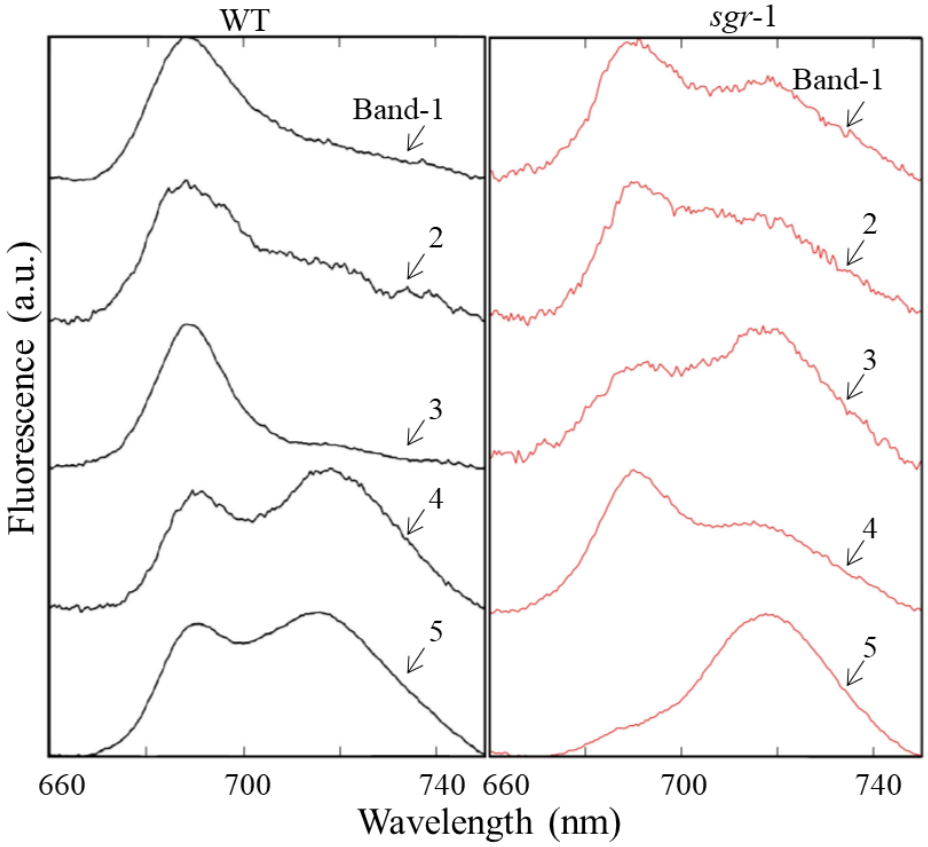

Fig. 13. Low temperature fluorescence spectra of the green bands resolved by BN-PAGE. Green bands 1 to 5 from Chlamydomonas WT and *sgr* mutant (*sgr*-1 mutant only, *sgr*-2 mutant showed similar results and data not shown) were excised and frozen in liquid nitrogen and kept in dark environment, and the fluorescence emission spectra at 440 nm excitation were directly measured in liquid nitrogen temperature. For each green band, the means of 60 spectra are presented.

3. 8. Silver Staining of BN-PAGE Bands of Chlamydomonas.

The primary conclusion of the low-temperature fluorescence of BN-PAGE bands is followed: band 1 to 5 showed strong signals of the PS systems super complex including PSI and PSII in WT but reduced PSII levels in Chlamydomonas *sgr* mutant (*sgr* mutant-1 only, *sgr* mutant-2 showed the similar results and data not shown). Band 6 and 7 showed a similar signal as LHCII trimer and monomer. These PSs identification were confirmed by silver staining of the individual green bands (Fig. 14).

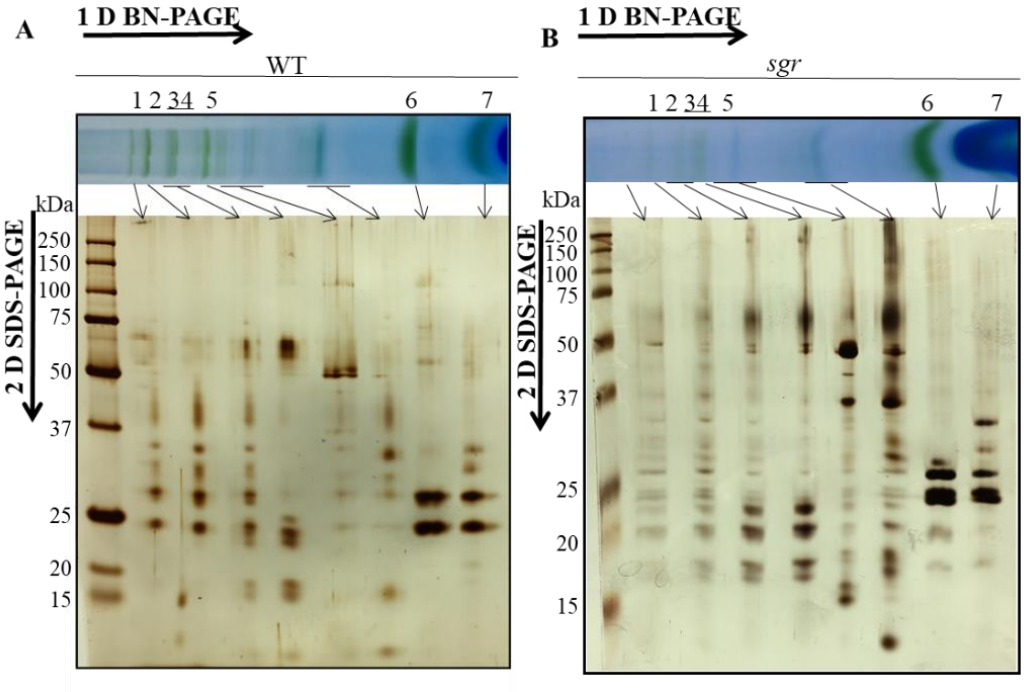

Fig. 14. Silver staining analysis of BN-PAGE of Chlamydomonas. Bands from the BN-PAGE gel of Chlamydomonas WT (A) and the *sgr* mutant (B) (the Chlamydomonas *sgr*-1 mutant only, the *sgr*-2 mutant showed similar result and data not shown) were excised and examined using SDS-PAGE. Silver staining were performed, loaded volume of marker for wild type and *sgr*-1 is 1 and 0.1 μ ml respectively.

3. 9. Immunoblotting Analysis of Chlamydomonas Protein.

To investigate each protein level of PSs, immunoblotting analysis (Fig. 15) was performed. Chlamydomonas WT protein was diluted from 1/4 to 1 time. Compared with the WT, both two Chlamydomonas *sgr* mutants showed reduced more than 75%

levels of PSII proteins. Interestingly, D2 protein levels were higher compared with other PSII proteins because the remained pre-assembly PSII component was similar as previously paper (Che et al., 2013). By contrast, PSI proteins and LHCII proteins levels were not particularly different between Chlamydomonas WT and *sgr* mutants. These results also indicate that PSII RC is preferentially reduced but PSI RC remained in Chlamydomonas *sgr* mutants, which is consistent with BN-PAGE analysis (Fig. 12).

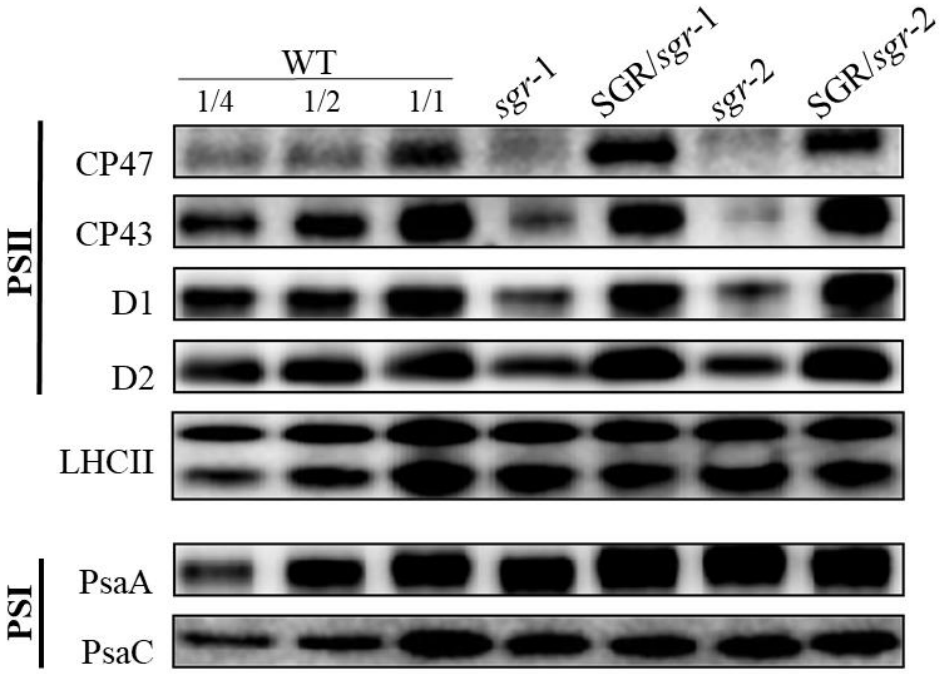

Fig. 15. Immunoblotting analysis of photosynthetic proteins of Chlamydomonas. Chlamydomonas cells were grown in TAP media at NL80, and membrane proteins containing 0.2 μg Chl (CP47, CP43, D1, PsaA, and PsaC) or 0.1 μg Chl (D2 and LHCII) were used for analyzing.

3. 10. Low-Temperature Fluorescence Analysis of Chlamydomonas Whole Cells.

To further examine the reduced PSII level, the low-temperature fluorescence spectra of Chlamydomonas whole cells were measured using Hitachi F-2500 Fluorescence Spectrophotometer (Fig. 16). The fluorescent peak around 710 nm was observed as the signal of PSI. Fluorescence spectra were normalized based on this peak. WT: *sgr* (the Chlamydomonas *sgr*-1 mutant only, the *sgr*-2 mutant showed similar result and

data not shown) mutant was compared at 680nm which is the signal of PSII. The PSII fluorescent peak of Chlamydomonas *sgr* mutant was only 70% of the WT, which indicate that the PSII level was reduced in Chlamydomonas *sgr* mutants. This result consists with the conclusion of BN-PAGE analysis results (Fig. 12) and immunoblotting analysis results (Fig. 15). It is further proved that the Chlamydomonas *SGR* is involved in PSII formation.

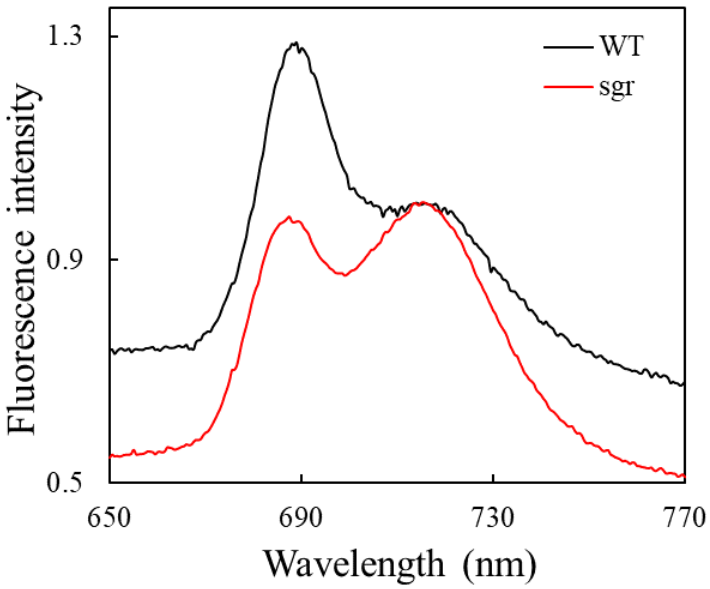

Fig. 16. Low temperature fluorescence spectra of the Chlamydomonas cells. Chlamydomonas cells were grown at NL80, and the fluorescence emission spectra at 440 nm excitation were directly measured in liquid nitrogen temperature. The fluorescence spectra were normalized at 710 nm, and the spectra are presented by the means of 20 times.

3. 11. P700/Chl Ratios Analysis of Chlamydomonas.

To further determine the PSI levels, P700/Chl ratios were measured using the spectroscopic method (Fig. 17). Chlamydomonas *sgr* mutants showed high P700/Chl level than WT. This is reasonable, because the Chl content (Fig. 11) was reduced compared to WT caused by PSII (Fig. 15, Fig. 16) lacking. From this result, the PSI level of *sgr* mutant was carried out, which is Chlamydomonas *SGR* is not involved in PSI formation.

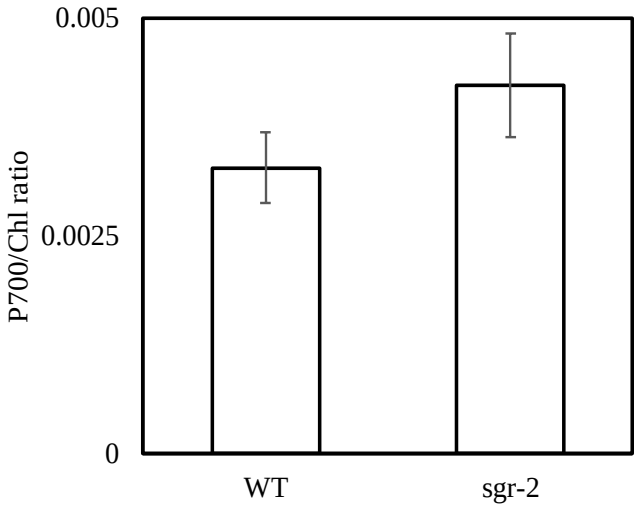

Fig. 17. P700/Chl ratios of Chlamydomonas. Chlamydomonas cells were grown in TAP media at NL80.

3. 12. Chl Degradation Analysis of Chlamydomonas.

Previously report (Park et al., 2007b) showed SGR catalyzes the first step of Chl degradation by converting Chl *a* to Pheo *a* in land plants, and Chl degradation was delayed in the Arabidopsis *sgr* triple mutant. The contribution of *SGR* to Chl degradation was examined. Instead of unwieldy senescence, Chl degradation was induced by nitrogen (N) starvation at photo mixotrophic culture conditions (Fig. 18).

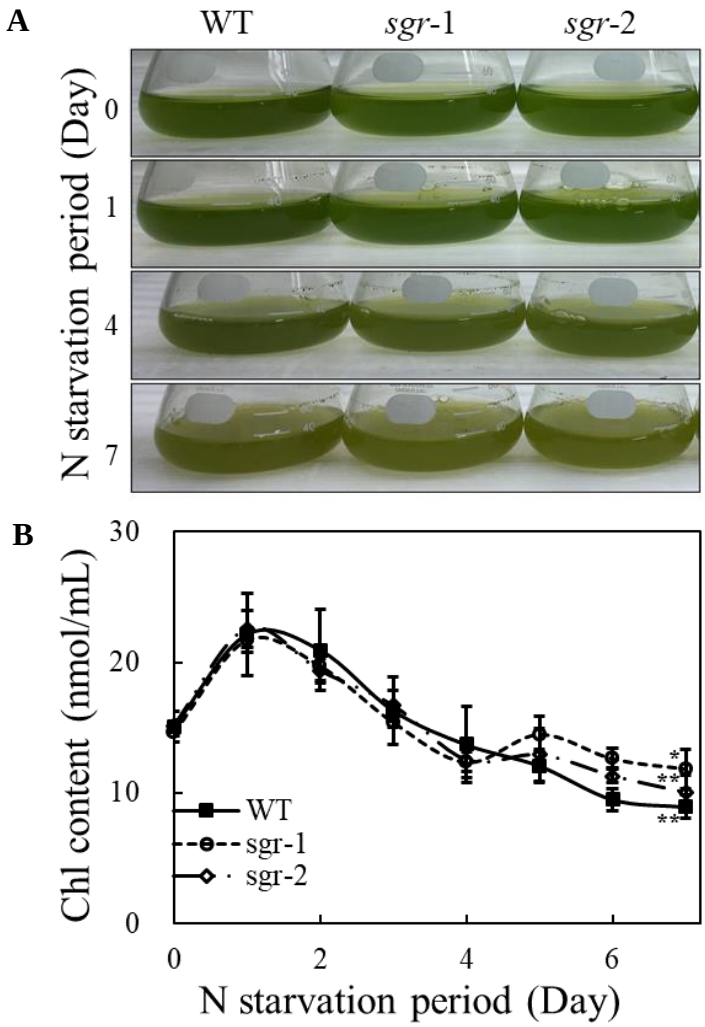

Fig. 18. Chl degradation during N starvation. Chlamydomonas cells were grown in TAP medium at NL80 and transferred to TAP-N- medium. (A) Pictures of cultures during nitrogen starvation. (B) Changes in the Chl content during nitrogen starvation. Measurements from 3–6 biological replicates (mean ± SD) that were significantly different between day 7 and day 1 are indicated (** $P < 0.01$, * $P < 0.05$, Student's t-test).

When the Chlamydomonas cells were transferred from N-plus to N-free medium, the Chl content transiently increased during the first day. One of the possible reasons is the Chl generation from precursor substance and then decrease for recycling N. After four days of N-starvation, the Chl degradation rate slowed and ceased, which is consistent with a previous study (Schelbert et al., 2009). Furthermore, The Chl degradation rates in the Chlamydomonas WT and two *sgr* mutants showed a similar tendency.

Chlamydomonas Chl degradation is more rapidly at photoautotrophic culture than

mixotrophic culture under nitrogen deprivation conditions (Schulz-Raffelt et al., 2016). N starvation at photoautotrophic culture condition was carried out. 5% CO_2 was continuously supplying as a carbon source. Around 65 and 70~75% of the Chl was degraded in the Chlamydomonas WT and the *sgr* mutants compared with the top levels, respectively (Fig. 19). These two experiment results (Fig. 18, Fig. 19) suggest that Chlamydomonas *SGR* (CrSGR) is not involved in Chl degradation.

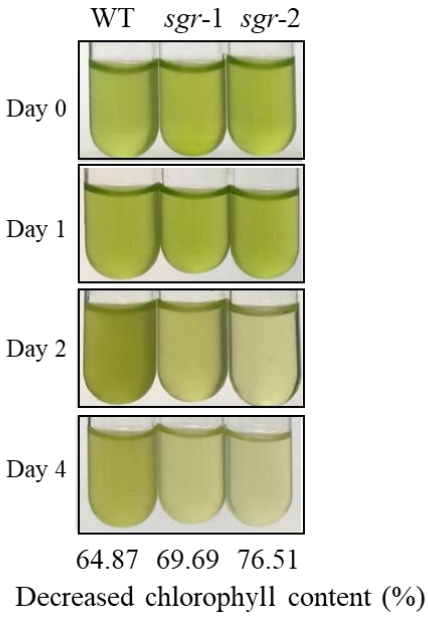

Fig. 19. Chl degradation under N starvation in photoautotrophic conditions. Chlamydomonas cells were grown in TAP media to logarithmic phase at NL80 and were transferred to TP-N- media with 5% CO_2 continuous positive airway pressure. Pictures of cultures during N starvation.

To investigate the change of related mRNA expression levels, qRT-PCR was carried out (Fig. 20). The pigments degradation was regulated and controlled by a number of genes, including NON-YELLOW COLORING1 (*NYC1*), pheophorbide *a* oxygenase (*PaO*). The expression levels of these genes are up-regulated during leaf senescence in the land plant (Sakuraba et al., 2007).

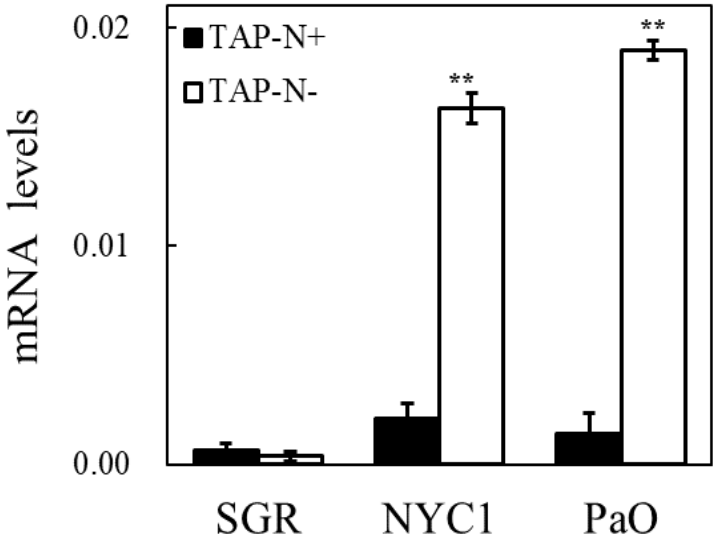

Fig. 20. Gene expression during nitrogen starvation. Relative mRNA expression levels of *SGR*, *NYC1* and *PaO* at the third day of nitrogen starvation. Measurements from 3–6 biological replicates (mean ± SD) that were significantly different between TAP-N- and TAP-N+ are indicated (** $P < 0.01$, Student's t-test). # *PaO* is closely related to a vascular plant PaOs, but it has not yet been enzymatically.

After three days of N starvation, the mRNA expression levels of both *NYC1* and *PaO* increased. However, the *SGR* mRNA expression level was reduced by N starvation. This is different from Arabidopsis which *SGR* mRNA expression level is up-regulated during Chl degradation (Sakuraba et al., 2012). These results indicate that Chlamydomonas *SGR* is not associated with Chl degradation.

3. 13. Life Span of Arabidopsis *sgr* Triple Mutant.

It had previously been cleared that SGR could catalyze Chl *a* degrade to Pheo *a*, which is a crucial and dispensable molecular in PSII reaction center, but whether Arabidopsis SGR is involved in PSII formation is still unclear. Arabidopsis *sgr* triple mutant is totally lacking *sgr 1*, *2* and *l* genes, was constructed to elucidate the physiological role of *SGR*. It is showed similar phenotype at a developmental stage (Fig. 21) with WT, which implies the normal formed PSs regulates by another Pheo *a* supply mechanism. At senescence stage, Arabidopsis *sgr* triple showed delayed Chl degradation and stay green phenotype (Fig. 21). This is consistent with the function of Arabidopsis *SGR* which is involved in Chl degradation.

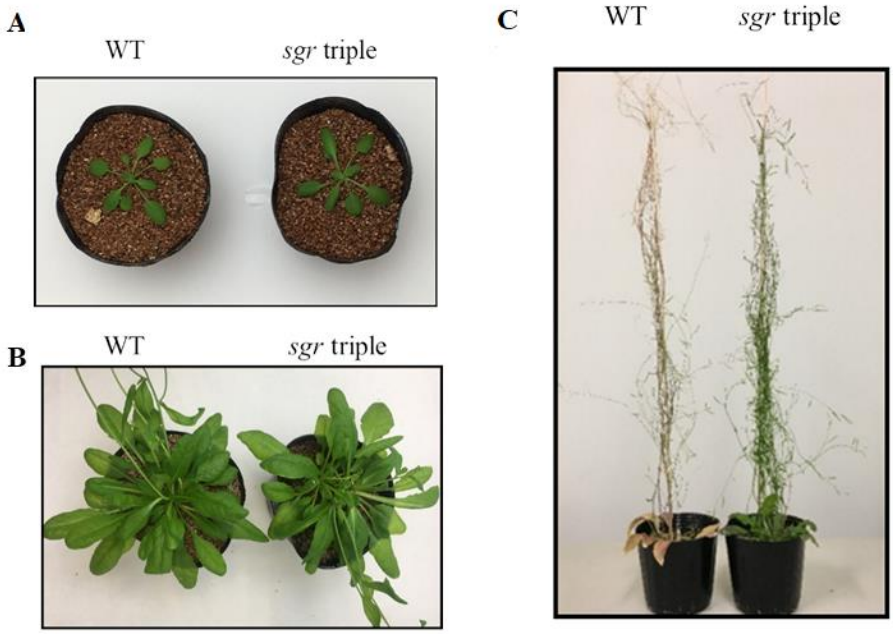

Fig. 21. Phenotypes of Arabidopsis *sgr* mutant during the life span. Arabidopsis plants grown under NL80 at 25 ℃. (A) Photograph of early developmental stage plants. (B) Photograph of developmental stage plants. (C) Photograph of natural senescence stage plants.

3. 14. Fv/Fm Ratios of Arabidopsis *sgr* Triple Mutant.

To figure out the PSII activity in the different stages, the Fv/Fm ratio was measured. Fv/Fm ratios (Fig. 22) at the developmental stage were similar in Arabidopsis WT and *sgr* triple mutants, indicating that Arabidopsis *SGR* is not involved in PSII formation. There must be another gene existed in Arabidopsis who involved in PSII formation and/or Pheo *a* supplying. However, it is shown that reduced Fv/Fm ratios in Arabidopsis *sgr* triple mutants at the senescence stage. This might be caused by the photodamage because the remained Chl absorbs the excess light energy.

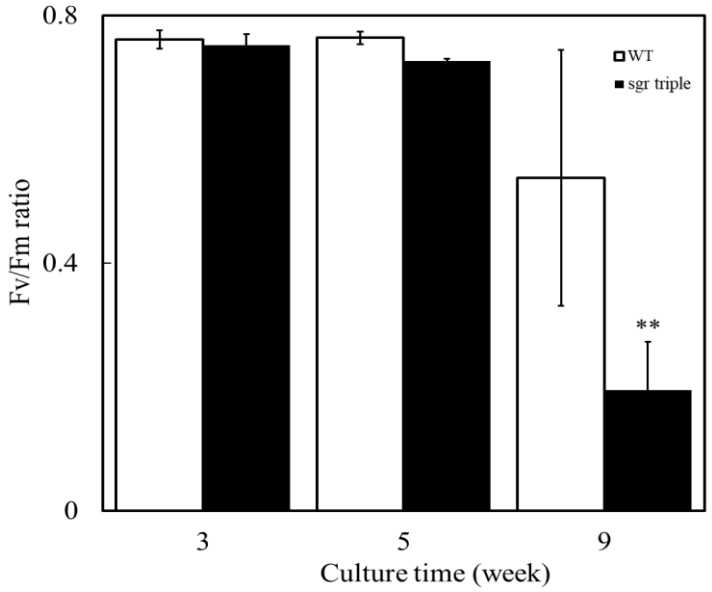

Fig. 22. Fv/Fm ratios of Arabidopsis during the life span. Arabidopsis plants grown at NL80 were measured after 10 min of dark acclimation. Measurements from 3 biological replicates (mean ± SD) that were significantly different from the WT are indicated (** $P < 0.01$, Student's t-test).

3. 15. The Pigment Analysis of Arabidopsis.

To further examine the function of Arabidopsis *SGR* in Chl degradation during senescence, the levels of major pigments were investigated. HPLC results confirmed the results of Fig. 21, Arabidopsis WT and *sgr* triple mutant showed similar pigments levels at the developmental stage but delayed pigment degradation after dark-induced senescence in the detached leaves (Table. 4). At the developmental stage, higher Chl level of Arabidopsis *sgr* triple mutant might be because of the higher accumulated Chl by photosynthesis and retained Chl degradation speed by *SGR* lacking. And the carotenes are slightly high in *sgr* triple mutants. Notably, the Pheo *a* level between Arabidopsis WT and *sgr* triple mutant were similar, even the *sgr* mutant could not degrade Chl *a* by SGR. This result implies another mechanism of Pheo *a* generation, which is Arabidopsis SGR is not the only way to generate Pheo *a* to supplying for PSII formation. After dark-induced senescence, Chl level of *sgr* triple mutant is extremely conserved because of the blocked Chl degradation pathway. The same phenotype was observed in the carotenes. These experiments indicate that Arabidopsis

SGR plays a crucial role in Chl degradation, which is consisted of the previous studies.

Table. 4 Pigments contents of Arabidopsis WT and *sgr* triple mutant.

Name		Chl *a* (nmol cm^{-2})	Chl *b* (nmol cm^{-2})	Pheo *a* (nmol cm^{-2})	Neo (area cm^{-2})	Viol (area cm^{-2})
Before dark incubation	WT	27.79±10.90	8.89±3.26	12.40±5.40	3654.60±1371.97	3077.30±1226.87
	sgr triple	32.48±5.71	9.51±1.73	12.40±5.40	3797.28±494.12	1398.36±615.61
After dark incubation	WT	2.82±0.65	0.78±0.17	12.40±5.40	399.92±88.97	898.81±169.15
	sgr triple	16.26±4.55	2.71±1.25	18.08±5.48	2240.54±573.01	1832.53±715.19

3. 16. PSII formation and the Pheo *a* Level.

PSII formation and the Pheo *a*/Chl ratios were significantly related in Chlamydomonas. This is because the Chlamydomonas *SGR* supply Pheo *a* to PSII formation. Arabidopsis *SGR* is involved in the Chl degradation by converting Chl *a* to Pheo *a* (Shimoda et al., 2016) but not involved in the PSII formation (Fig. 22). The Pheo *a* level of developmental stage Arabidopsis and *sgr* triple mutant are similar. This phenotype could further support the hypothesis that PSII formation is affected by Pheo *a* supply. Because of the abundant Pheo *a* supply, PSII formation could normally be synthesized. At senescence stage, the Pheo *a* level of *sgr* triple mutant is higher than WT. This is because Chl degradation in *sgr* triple mutant is blocked. The reduced Chl degradation intermediates could not give enough signal to upregulate the whole degradation procedure. This could further delay of Chl degradation to kept higher pigments amount including Pheo *a* and retained membrane structure containing PSs complex.

3. 17. The Immunoblotting Analysis of Arabidopsis Protein.

Fv/Fm ratio (Fig. 22) of Arabidopsis *sgr* triple mutants showed the standard Fv/Fm

ratios at the developmental stage, which imply the unaffected PSII activity. To further certify the role of Arabidopsis *SGR* in PSII formation, immunoblotting analysis were performed to analyze the individual PSs proteins levels (Fig. 23). Arabidopsis WT and *sgr* triple mutants showed similar levels of PSI, PSII and LHCII proteins, indicating that Arabidopsis *SGR* is not functional to PSs formation.

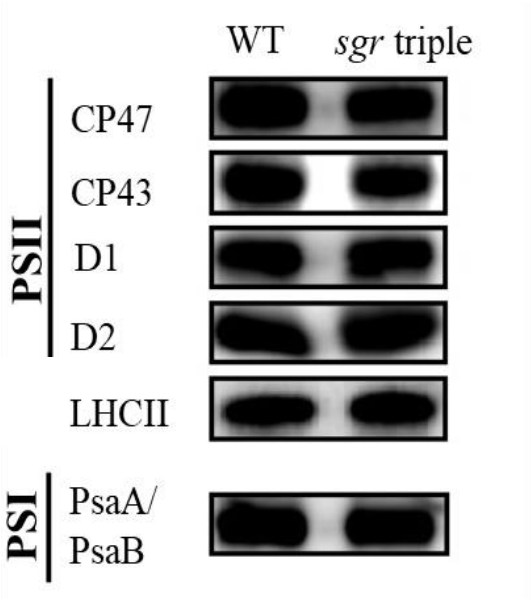

Fig. 23. Immunoblotting analysis of Arabidopsis. Arabidopsis plants were grown under NL80, and photosynthetic proteins isolated from developmental stage plants leaves. Membrane proteins containing 0.2 μg Chl (CP47, CP43, D1, PsaA/B) or 0.1 μg Chl (D2 and LHCII) were used for analyzing.

3. 18. The BN-PAGE Analysis of Arabidopsis Protein.

To further investigate the PSII and PS SC complex levels and further verify the function of Arabidopsis *SGR*, BN-PAGE analysis (Fig. 24) was performed. The result showed that before dark incubation, the PSs protein levels in developmental stage WT and *sgr* triple mutant were similar, which is consistent with Fv/Fm ratios (Fig. 22) and immunoblotting analysis (Fig. 23) results. After 6 days dark incubation, proteins, and pigments in PSs SC were sharply and almost all degraded in WT but slightly remained in *sgr* triple mutant. It means the Arabidopsis *SGR* is involved in the PSs protein-pigment complex degradation consistent with the previous report (Shimoda et al., 2016).

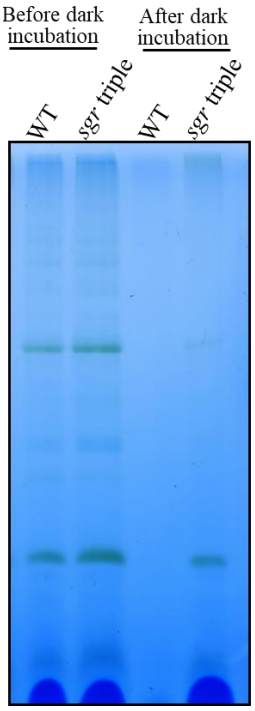

Fig. 24. BN-PAGE analysis of Arabidopsis. Arabidopsis plants were grown at NL80, detached leaves from developmental stage plants were sealed and dark incubated for 6 days, and the PSs proteins were resolved to perform BN-PAGE.

3. 19. Complementation and Isolation of Arabidopsis CrSGR Lines.

CrSGR has the same catalytic properties (Matsuda et al., 2016) as Arabidopsis SGR (AtSGR) 1 transiently expressed CrSGR induced Chl degradation in Arabidopsis. In this study, CrSGR was constitutively expressed in an Arabidopsis *sgr* triple mutant using 35S promoter (CrSGR-35S) or an Arabidopsis native promoter (which is 2 kbp upstream of AtSGR1) (CrSGR-N).

Arabidopsis CrSGR complementation showed low germination rate, delayed growth speed, paled leaves and easy death (data not shown). All these phenotypes were caused by the CrSGR gene insertion. Basta spray screening results showed more than half plants were death in T2, this result does not agree with Mendel's law of inheritance. The Arabidopsis CrSGR complementation lines plants showed the same phenotype and remarkable death rate during plant development without basta spray. From these results, it was expected that the complementation plants with high expression CrSGR level were not survived. Therefore, the complementation plants

with low expression CrSGR levels should be selected. Genomic PCR was performed to further identify the Arabidopsis CrSGR-35S and CrSGR-N complementation lines. The Arabidopsis CrSGR complementation lines are confirmed by genomic PCR (Fig. 25).

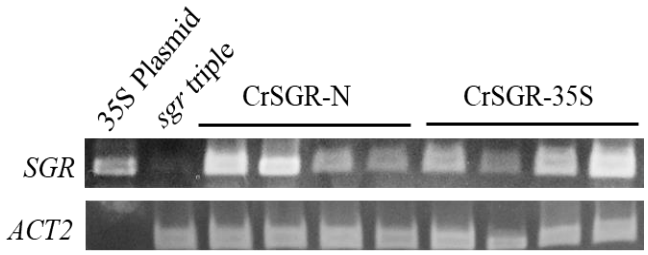

Fig. 25. Genomic PCR of confirmation Arabidopsis CrSGR complementation lines. 35S promoter plasmid was used the positive control.

3. 20. Chl Degradation Analysis of CrSGR Complementation Lines.

To investigate the catalytic properties of CrSGR, dark incubated senescence of detached leaves was performed. The Arabidopsis *sgr* triple mutants exhibited the stay-green phenotype, while the detached leaves of the WT turned yellow after 10 days dark incubation. The detached leaves of Arabidopsis CrSGR-N and CrSGR-35S complementation lines only slightly turned yellow after dark incubation (Fig. 26).

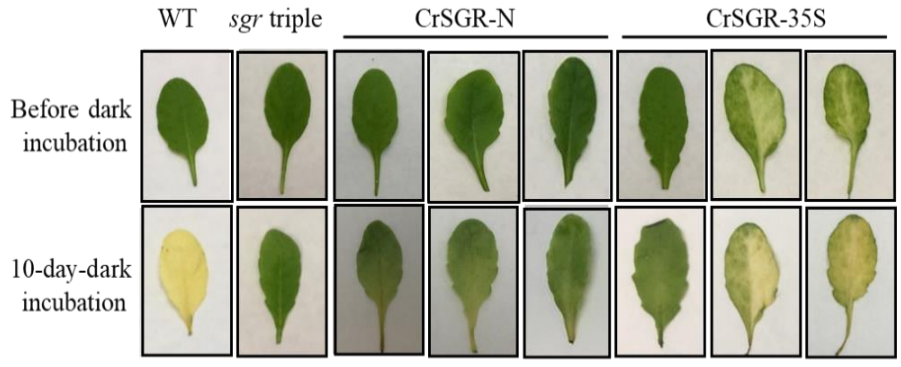

Fig. 26. Dark-induced senescent leaves of the Arabidopsis CrSGR complementation lines. Three-week-old Arabidopsis detached leaves were incubated in the dark for 10 days.

Under natural senescence (Fig. 27), the Arabidopsis *sgr* triple mutants retained the

stay-green phenotype, while the WT turned yellow at the senescence stage. CrSGR-N and CrSGR-35S only slightly turned yellow as same as dark-induced senescence of detached-leaves.

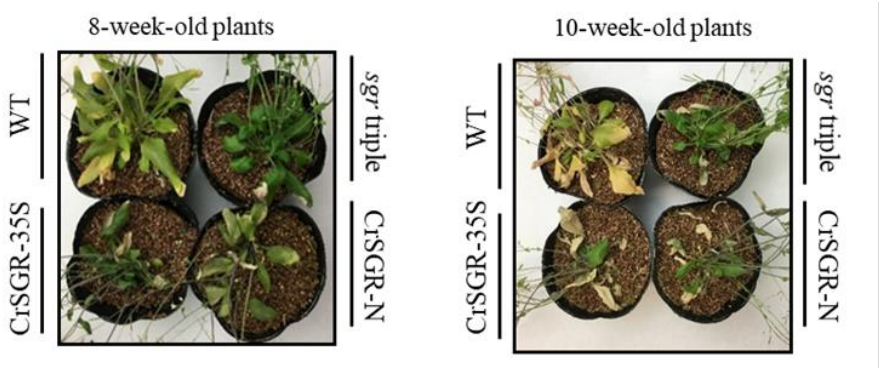

Fig. 27. Dark-induced senescent plants of the Arabidopsis CrSGR complementation lines.

All these experiments results indicate that CrSGR partly rescues the Arabidopsis *sgr* phenotypes. The possible reason of the only partly rescued phenotype is the selection strategy. On transiently expressed complementation lines screening, the high expressed complementation lines were screened (Matsuda et al., 2016). Different from the screening strategy of transient expression, only the lower expressed constitutively complementation lines could be selected. The partly rescued phenotypes of Arabidopsis CrSGR complementation lines are accepted. It appears that SGR is associated with different physiological processes in Arabidopsis and Chlamydomonas, despite having the same catalytic properties.

4. Discussion

4.1. Chlamydomonas Stay-Green (*SGR*) is Functional in Photosystem (PS) II Formation by Supplying Pheophytin (Pheo) *a*.

Chlamydomonas *sgr* mutant isolation is based on the hypothetical function of SGR, which is for PSII formation by supply Pheo *a*. Based on the previously report (Sirpiö et al., 2008; Zhang et al., 2010) that the possible mechanism for the low maximum quantum efficiency of PSII (Fv/Fm) ratio is a defect in the assembly of PSII, the Chlamydomonas *sgr* null mutants were successfully obtained by lower Fv/Fm ratios screening and confirmed by genomic PCR (Fig. 4). Additionally, the Fv/Fm ratio of Chlamydomonas *sgr* mutants under low light conditions (1 μmol photon m^{-2} s^{-1}, LL1) and normal light condition (80 μmol photons m^{-2} s^{-1}, NL80) have high consistency, which indicates the reduced Fv/Fm ratio in Chlamydomonas *sgr* mutants were not caused by photodamage. Furthermore, all these Chlamydomonas lines showed reduced Fv/Fm ratios (and never recovered in SL750 for *sgr* mutants) including WT under high light conditions (250 μmol photons m^{-2} s^{-1}, HL250) (Fig. 5) and strong light conditions (750 μmol photons m^{-2} s^{-1}, SL750) (Fig. 6), which means the active PSII in Chlamydomonas *sgr* mutants are weakened by *SGR* gene deletion.

The lower growth speed of the Chlamydomonas *sgr* mutant at photo mixotrophically (Fig. 7) and photo autotrophically (Fig. 8) conditions means the restricted but existed PS activity that is consistent with the Fv/Fm ratios (Fig. 5). The Fv/Fm ratio of Chlamydomonas *sgr* mutant did not reach 0 at NL80 but remained almost half without any already known *sgr* homologous genes, which means the active PSII formation was not completely blocked but partly formed in the Chlamydomonas *sgr* mutants (Fig. 5) by the unclear reasons. One of the possible reasons is there is a second gene related to the PSII formation and Pheo *a* supplying.

Pheo *a* binds to D1 and D2 protein in the reaction center (RC) (Zabelin et al., 2014). Although the D2 protein levels (Fig. 15) were less than 25% in Chlamydomonas *sgr* mutants compared with WT, the Pheo *a* level (Fig. 9) were remained 60% of the wild type (WT), suggesting that Pheo *a* is synthesized by other mechanisms or created by Chl *a* degradation. This is consistent with the half remained Fv/Fm ratio in null *sgr* mutant. The redundant Pheo *a* existing in the cell as free-Pheo *a* or Pheo *a* which

binding to the pre-assembly PSII component, and it is not efficiently used for active PSII formation. The Pheo *a*/Chl ratio determined using high-performance liquid chromatography (HPLC) in this study is different from the value determined using an optical method (Guenther et al., 1990), suggesting the accumulation of nonfunctional Pheo *a*.

This hypothesis is supported by the Pheo *a*/Chl ratios of *psb*D mutant (Fig. 10) which does not contain PSII (Erickson et al., 1986) is around 0.005-0.007, which has the similar Pheo *a* level with the Chlamydomonas *sgr* mutant. The existence of the Pheo *a* unbound to PSII could be one of the reasons for the discrepancy between D1 and Pheo *a* content of the Chlamydomonas WT and *sgr* mutants.

4.2. Chlamydomonas *SGR* is Functional in PSII but not in PSI and LHCII Formation.

Based on the partly remained PSII activity and the reduced Pheo a/Chl ratio of Chlamydomonas *sgr* mutants, it was considered as reduced PSII level. More experiments have been carried out to investigate the formation of PSs complex. Blue native polyacrylamide gel electrophoresis (BN-PAGE) analysis (Fig. 12) showed the reduced PSs SC levels of Chlamydomonas *sgr* mutant. This is further confirmed by silver staining (Fig. 14) and low-temperature fluorescence of BN-PAGE bands (Fig. 13) and of whole cells (Fig. 16). Results showed that PSII levels are reduced but PSI and LHCII remained. Immunoblotting analysis (Fig. 15) results showed the extremely reduced PSII levels and its components (D1, D2, CP43, and CP47) levels in Chlamydomonas *sgr* mutants. Based on these experiments, it is concluded Chlamydomonas *SGR* is contributed to the formation of PSII but not to PSI and LHCII formation.

Considering the similar Pheo *a*/Chl ratios (Fig. 9, Fig. 10) between Chlamydomonas *psbD* mutants and *sgr* mutants, which means the PSII level of Chlamydomonas *sgr* mutants is extremely low. This is proved by the partly remained PSII active (Fig. 5, Fig. 7, Fig. 8) and weakly repaired PSII (Fig. 6) of Chlamydomonas *sgr* mutants. These results showed that PSII formation was not completely blocked in the

Chlamydomonas *sgr* mutants (Fig. 15), which means the Pheo *a* in the Chlamydomonas *sgr* mutant could be formed by other mechanisms.

4.3. Pheo *a* Supply Strategy during PSII Formation and Repair.

PSII is the primary photon receptor and the electron donor for PSI. It is the major part to be photodamaged in PSs. The PSII assembly and disassembly/repair are very crucial processes that are regulated by many factors (Nickelsen and Rengstl, 2013; Theis and Schroda, 2016). During these processes, the Pheo *a* pool was prepared in the tissues of photosynthetic organisms, including the wasted Pheo *a* bound to the damaged D1 and will be degraded during the degradation of D1. The new Pheo *a* was produced for binding the new D1 proteins. The Pheo *a* pool of PSII deficient mutants testify the Pheo *a* total content by Chl degradation (Fig. 10).

This Pheo *a* supply must be strictly regulated by some regulatory mechanism because of the limited Pheo *a* would lead to reduced PSII level, and the excess Pheo *a* would toxic to cells and Chl *a* waste. One of the ideas of how to maintain the stable Pheo *a* supplying was the spontaneous response——Pheo *a* by spontaneous Mg release from Chl *a* under acidic conditions. Without question, maintaining this balance of Pheo *a* supplying is difficult. There might be another regulatory mechanism not to be illuminated yet. At the same time, the possibility of the second unidentified Mg-dechelatase cannot be evacuated.

4.4. Chlamydomonas *SGR* was not Associated with Chl Degradation.

The first step of Chl degradation is the conversion of Chl *a* to Pheo *a* by extracting Mg from the center of Chl *a* (Hörtensteiner, 2006). During leaf senescence, proteins and Chl is degraded to recycle nutrient (Gregersen et al., 2008), the expression level of Chl degradation related genes are up-regulated (Pruzinska et al., 2003). The *sgr* mutants of various land plants have a delayed Chl-degradation phenotype (Cha et al., 2002; Armstead et al., 2007b; Barry et al., 2008; Zhou et al., 2011).

Similar to leaf senescence, the green algae cultured under nitrogen deprivation conditions also showed proteins and Chl degradation phenotype (Schmollinger et al., 2014). However, in this study, the Chl degradation rates in green algae——Chlamydomonas were not particularly different between the *sgr* mutants and the WT (Fig. 18, Fig. 19). This result strongly supports the idea that Chlamydomonas *SGR* is not functional in Chl degradation. Interestingly, unlike other Chl-degradation enzymes, including pheophorbide *a* oxygenase (PaO) and Chl *b* reductase (NYC1) (Fig. 20) (Kuai et al., 2018), *SGR* (Fig. 20) was not up-regulated during N starvation since the Chl began to be degraded. This result suggests that *SGR* is not involved in Chl degradation in Chlamydomonas.

However, it should be noted that the substrates of pheophytinase (PPH) (Chen et al., 2016) and PaO in the Chl-degradation pathway are Pheo *a* and pheophorbide (Pheide) *a*, respectively. These molecules have no central magnesium (Mg). Therefore, in Chlamydomonas, the Mg molecules must have been removed before the reactions that are catalyzed by PPH and PaO. This phenomenon could be explained by the existence of a second Chl degrading Mg-dechelatase in Chlamydomonas.

4.5. Arabidopsis *SGR* is not Functional in PSII Formation but in Chl Degradation.

The physiological functions of *SGR* have been extensively studied in vascular plants (Bell et al., 2015; Yasuhito et al., 2015; Qian et al., 2016). Without exception, the Arabidopsis *sgr* triple mutant had a strong stay-green phenotype (Fig. 21), which is consistent with the fact that SGR catalyzes the first and committed step of Chl degradation.

There are three *SGR* genes in the Arabidopsis genome: *SGR1*, *SGR2,* and *SGRL* (Yasuhito et al., 2015; Shimoda et al., 2016). *SGR1* and *SGR2* are expressed during senescence, and the *sgr1*/*2* double mutant shows a strong stay-green phenotype (Wu et al., 2016). These results indicate that *SGR1* and *SGR*2 are responsible for Chl degradation during senescence, which is consistent with the mRNA expression levels during the life span of vascular plants (Balazadeh, 2014). By contrast, *SGRL* is

primarily expressed in green tissues and is significantly down-regulated in leaves undergoing natural and dark-induced senescence, which implies *SGRL* is not involved in Chl degradation at the senescence stage. Additionally, all higher plants contain at least one *SGRL* (Yasuhito et al., 2015), indicating that *SGRL* has essential functions in green plants. *SGRL* is possibly involved in photoprotection (Bell et al., 2015) or abiotic stress (Sakuraba et al., 2014) and Chl degradation (Rong et al., 2013).

Although the *SGRL* expression pattern suggests its involvement in PSII formation, the PSII level and the Fv/Fm ratio of the Arabidopsis *sgr* triple mutant were the same as those of the WT (Fig. 22). These results suggesting that Arabidopsis *SGR* is not contributed to PSII formation which is different from Chlamydomonas *SGR*. The functional differences of *SGR* in the green plant Arabidopsis and green algae Chlamydomonas might be because of the evolutionary differences.

4.6. The Secondly Mg-dechelatase Possible Exists from Cyanobacteria to Green Plants.

It should be noted that AtSGR1 (Shimoda et al., 2016) and CrSGR (Matsuda et al., 2016) catalyze the same reaction that converts Chl *a* to Pheo *a* rather than converts chlorophyllide (Chlide) *a* to Pheide *a*. Furthermore, *CrSGR* partly complemented the Arabidopsis *sgr triple* mutants (Fig. 26, Fig. 27) and transiently expressed *CrSGR* in Arabidopsis induced Chl degradation (Matsuda et al., 2016). These results indicate that the enzymatic properties between AtSGR and CrSGR are identical, but the physiological functions are different. One of the possible reasons for this difference is other mechanisms such as the enzyme localization.

These results also suggest that another unidentified Mg-dechelatase possibly exist both in Arabidopsis and Chlamydomonas. The Arabidopsis *sgr* triple mutant who completely lacking *sgr 1*, *2*, *l*, but the PSII could normally form. It is implying the normal supplied Pheo *a* without Arabidopsis *SGR*. This could be explained by an unknown Mg-dechelatase who could supply Pheo *a* to PSII formation. The Chlamydomonas *sgr* mutant has half remained PSII activity with half amount Pheo *a* supplying, and similar degraded Chl compared with WT. These results implying the

second Mg-dechelatase who involve in Chl degradation to supplying Pheo *a* for PSII formation. Photosynthetic organisms other than green plants which located at the bottom of the evolutionary niche, such as red algae (Gardian et al., 2007) and cyanobacteria (Watanabe et al., 2014), do not possess *SGR*, but still could degrade Chl (Murakami et al., 2004; Vavilin and Vermaas, 2007) and form PSII (Kondo et al., 2007; Neilson and Durnford, 2010; Heinz et al., 2016). Therefore, the possibility of another unidentified Mg-dechelatase existence in red algae and cyanobacteria cannot be excluded. It might be associated with PSII formation and Chl degradation just like the first Mg-dechelatase (Rong et al., 2013; Yasuhito et al., 2015; Matsuda et al., 2016; Shimoda et al., 2016). This unidentified Mg-dechelatase could also be a candidate for the second Mg-dechelatase in green plants.

4.7. SGR Physiological Function is Different Between Arabidopsis and Chlamydomonas.

All the data showed that the Arabidopsis *SGR* is involved in Chl degradation (Shimoda et al., 2016), while the Chlamydomonas *SGR* participates in PSII formation. It is mentioned that SGR protein binds to LHCII where the major Chl locate, to execute the Chl degradation (Thomas and Ougham, 2014). In Arabidopsis, *SGR* and *NYC1* are associated with Chl degradation in the core and peripheral antenna complexes for Chl *a* and *b* degradation, respectively. The question arises as to why Chlamydomonas *SGR* is not involved in Chl degradation.

Green plants are divided into two groups including chlorophytes and streptophytes (Becker and Marin, 2009). Chlorophytes initially evolved in the deep sea (Leliaert et al., 2011), and early branching chlorophytes have Chl *b* not only in the LHC but also in the core antenna complexes (Kunugi et al., 2016). As shown previously, SGR does not extract Mg from Chl *b* (Shimoda et al., 2016), suggesting that SGR cannot efficiently degrade Chl in the core antenna complexes when they contain Chl *b*. This assumption is consistent with the result that Arabidopsis transgenic plants with core antennae containing Chl *b* have a stay-green phenotype that is indicative of delayed Chl degradation (Sakuraba et al., 2012).

Although Chlamydomonas does not have Chl *b* in its core antenna complexes, its progenitor had Chl *b*, and our results imply that it would not have been able to use *SGR* to degrade Chl. This characteristic is likely to have been inherited by Chlamydomonas. By contrast, Chl *b* is not present in the core antenna complexes of streptophytes, including Arabidopsis, and SGR can degrade all the Chl in the core antennae, which might be one of the reasons why *SGR* has different physiological functions between Arabidopsis and Chlamydomonas.

References

Alizadeh D, Cohen A (2010) Red Light and calmodulin regulate the expression of the psbA binding protein genes in chlamydomonas reinhardtii. Plant Cell Physiol **51**: 312–322

Alos E, Roca M, Iglesias DJ, Minguez-Mosquera MI, Damasceno CM, Thannhauser TW, Rose JK, Talon M, Cercos M (2008) An evaluation of the basis and consequences of a stay-green mutation in the navel negra citrus mutant using transcriptomic and proteomic profiling and metabolite analysis. Plant Physiol **147**: 1300–1315

Armstead I, Donnison I, Aubry S, Harper J, Hörtensteiner S, James C, Mani J, Moffet M, Ougham H, Roberts L, et al (2007a) Cross-Species Identification of Mendel's I Locus. Science (80-) **315**: 73

Armstead I, Donnison I, Aubry S, Harper J, Hörtensteiner S, James C, Mani J, Moffet M, Ougham H, Roberts L, et al (2007b) Cross-species identification of Mendel's/locus. Science (80-) **315**: 73

Balazadeh S (2014) Stay-green not always stays green. Mol Plant **7**: 1264–1266

Barros T, Kühlbrandt W (2009) Crystallisation, structure and function of plant light-harvesting Complex II. Biochim Biophys Acta - Bioenerg **1787**: 753–772

Barry CS, McQuinn RP, Chung MY, Besuden A, Giovannoni JJ (2008) Amino acid substitutions in homologs of the STAY-GREEN protein are responsible for the green-flesh and chlorophyll retainer mutations of tomato and pepper. Plant Physiol **147**: 179–187

Barry CS, Pandey P (2009) A survey of cultivated heirloom tomato varieties identifies four new mutant alleles at the green-flesh locus. Mol Breed **24**: 269–276

Barth C (2004) The Timing of Senescence and Response to Pathogens Is Altered in the Ascorbate-Deficient Arabidopsis Mutant vitamin c-1. Plant Physiol **134**: 1784–1792

Becker B, Marin B (2009) Streptophyte algae and the origin of embryophytes. Ann Bot **103**: 999–1004

Beisel KG, Jahnke S, Hofmann D, Köppchen S, Schurr U, Matsubara S (2010) Continuous Turnover of Carotenes and Chlorophyll a in Mature Leaves of Arabidopsis Revealed by 14CO2 Pulse-Chase Labeling. Plant Physiol **152**: 2188–2199

Bell A, Moreau C, Chinoy C, Spanner R, Dalmais M, Le Signor C, Bendahmane

A, Klenell M, Domoney C (2015) SGRL can regulate chlorophyll metabolism and contributes to normal plant growth and development in Pisum sativum L. Plant Mol Biol **89**: 539–558

Borrell AK, Mullet JE, George-Jaeggli B, Van Oosterom EJ, Hammer GL, Klein PE, Jordan DR (2014) Drought adaptation of stay-green sorghum is associated with canopy development, leaf anatomy, root growth, and water uptake. J Exp Bot **65**: 6251–6263

Casazza AP, Szczepaniak M, Müller MG, Zucchelli G, Holzwarth AR (2010) Energy transfer processes in the isolated core antenna complexes CP43 and CP47 of photosystem II. Biochim Biophys Acta - Bioenerg **1797**: 1606–1616

Cha KW, Lee YJ, Koh HJ, Lee BM, Nam YW, Paek NC (2002) Isolation, characterization, and mapping of the stay green mutant in rice. Theor Appl Genet **104**: 526–532

Che Y, Fu A, Hou X, McDonald K, Buchanan BB, Huang W, Luan S (2013) C-terminal processing of reaction center protein D1 is essential for the function and assembly of photosystem II in Arabidopsis. Proc Natl Acad Sci **110**: 16247–16252

Chen J, Ren G, Kuai B (2016) The Mystery of Mendel's Stay-Green: Magnesium Stays Chelated in Chlorophylls. Mol Plant **9**: 1556–1558

Cheung AY, McNellis T, Piekos B (1993) Maintenance of Chloroplast Components during Chromoplast Differentiation in the Tomato Mutant Green Flesh. Plant Physiol **101**: 1223–1229

Christ B, Hörtensteiner S (2014) Mechanism and Significance of Chlorophyll Breakdown. J Plant Growth Regul **33**: 4–20

Cogdell RJ, Gardiner AT, Cronin L (2012) Learning from photosynthesis: How to use solar energy to make fuels. Philos Trans R Soc A Math Phys Eng Sci **370**: 3819–3826

Cowgill J, Redding K, Jones A, Fromme P (2012) Characterization of the electron acceptors of the Type-I photosynthetic reaction center of *Heliobacterium modesticaldum*.

Dall'Osto L, Bressan M, Bassi R (2015) Biogenesis of light harvesting proteins. Biochim Biophys Acta - Bioenerg **1847**: 861–871

Danielsson R, Suorsa M, Paakkarinen V, Albertsson P-ÅÅ, Styring S, Aro E-MM, Mamedov F (2006) Dimeric and Monomeric Organization of Photosystem

II: DISTRIBUTION OF FIVE DISTINCT COMPLEXES IN THE DIFFERENT DOMAINS OF THE THYLAKOID MEMBRANE. J Biol Chem **281**: 14241–14249

Dekker JP, Boekema EJ (2005) Supramolecular organization of thylakoid membrane proteins in green plants. Biochim Biophys Acta **1706**: 12–39

Delmas F, Sankaranarayanan S, Deb S, Widdup E, Bournonville C, Bollier N, Northey JGB, McCourt P, Samuel MA (2013) ABI3 controls embryo degreening through Mendel's I locus. Proc Natl Acad Sci. doi: 10.1073/pnas.1308114110

Dewez D, Park S, Garcia-Cerdan JG, Lindberg P, Melis A, Oa PCW, Lindberg P, Melis A, Dewez D, Park S, et al (2009) Mechanism of REP27 Protein Action in the D1 Protein Turnover and Photosystem II Repair from Photodamage. Plant Physiol **151**: 88–99

Erickson JM, Rahire M, Malnoe P, Girard-Bascou J, Pierre Y, Bennoun P, Rochaix JD (1986) Lack of the D2 protein in a Chlamydomonas reinhardtii psbD mutant affects photosystem II stability and D1 expression. Embo J **5**: 1745–1754

Finazzi G, Drapier D, Rappaport F, Introduction I The CF 0 F 1 ATP Synthase Complex of Photosynthesis C H A P T E R C O N TE N T S. 639–670

Fristedt R, Vener A V (2011) High light induced disassembly of photosystem II supercomplexes in Arabidopsis requires STN7-dependent phosphorylation of CP29. PLoS One **6**: e24565

Fromme P, Jordan P, Krauß N (2001) Structure of photosystem I. Biochim Biophys Acta - Bioenerg **1507**: 5–31

Fu J, Lee B, Lee B (2000) Changes in Photosynthetic Characteristics during Grain Filling of a Functional Stay-Green Rice SNU- SG1 and its F 1 Hybrids * To whom correspondence should be addressed. **11**: 75–82

Fukao T, Yeung E, Bailey-Serres J (2012) The Submergence Tolerance Gene SUB1A Delays Leaf Senescence under Prolonged Darkness through Hormonal Regulation in Rice. Plant Physiol **160**: 1795–1807

Gan S, Amasino RM (1995) Inhibition of leaf senescence by autoregulated production of cytokinin. Science (80-) **270**: 1986–1988

García-Cerdán JG, Kovács L, Tõth T, Kereïche S, Aseeva E, Boekema EJ, Mamedov F, Funk C, Schröder WP (2011) The PsbW protein stabilizes the

supramolecular organization of photosystem II in higher plants. Plant J **65**: 368–381

Gardian Z, Bumba L, Schrofel A, Herbstova M, Nebesarova J, Vacha F (2007) Organisation of Photosystem I and Photosystem II in red alga Cyanidium caldarium: Encounter of cyanobacterial and higher plant concepts. Biochim Biophys Acta - Bioenerg **1767**: 725–731

Garnier J, Wu B, Jeannine M, Guyon D, Trémolières A (1990) Restoration of both an oligomeric form of the light-harvesting antenna CP II and a fluorescence state II-state I transition by Δ3-trans-hexadecenoic acid-containing phosphatidylglycerol, in cells of a mutant of Chlamydomonas reinhardtii. BBA - Bioenerg **1020**: 153–162

Gregersen PL, Holm PB, Krupinska K (2008) Leaf senescence and nutrient remobilisation in barley and wheat. Plant Biol **10**: 37–49

Guenther JE, Nemson JA, Melis A (1990) Development of Photosystem II in dark grown Chlamydomonas reinhardtii. A light-dependent conversion of PS IIβ, QB-nonreducing centers to the PS IIα, QB-reducing form. Photosynth Res **24**: 35–46

Guiamét JJ, Tyystjärvi E, Tyystjärvi T, John I, Kairavuo M, Pichersky E, Noodén LD, Guiamet JJ, Tyystjarvi E, Tyystjarvi T, et al (2002) Photoinhibition and loss of photosystem II reaction centre proteins during senescence of soybean leaves. Enhancement of photoinhibition by the "stay-green" mutation cytG. Physiol Plant **115**: 468–478

Hatano-Iwasaki A, Minagawa J, Inoue Y, Takahashi Y (2000) Characterization of chloroplast psbA transformants of Chlamydomonas reinhardtii with impaired processing of a precursor of a photosystem II reaction center protein, D1. Plant Mol Biol **42**: 353–63

Heinz S, Liauw P, Nickelsen J, Nowaczyk M (2016) Analysis of photosystem II biogenesis in cyanobacteria. Biochim Biophys Acta - Bioenerg **1857**: 274–287

Henderson JN, Zhang J, Evans BW, Redding K (2003) Disassembly and degradation of photosystem I in an in vitro system are multievent, metal-dependent processes. J Biol Chem **278**: 39978–39986

Hohmann-Marriott MF, Blankenship RE (2011) Evolution of photosynthesis. Annu Rev Plant Biol **62**: 515–548

Hoober JK, Eggink LL, Chen M (2007) Chlorophylls, ligands and assembly of light-harvesting complexes in chloroplasts. Photosynth Res **94**: 387–400

Hörtensteiner S (2006) Chlorophyll Degradation During Senescence. Annu Rev Plant Biol **57**: 55–77

Hörtensteiner S (2009) Stay-green regulates chlorophyll and chlorophyll-binding protein degradation during senescence. Trends Plant Sci **14**: 155–162

Hörtensteiner S (2012) Update on the biochemistry of chlorophyll breakdown. Plant Mol Biol 1–13

Hörtensteiner S, Krautler B, Kräutler B (2011) Chlorophyll breakdown in higher plants. Biochim Biophys Acta - Bioenerg **1807**: 977–988

Hu Y, Jiang Y, Han X, Wang H, Pan J, Yu D (2017) Jasmonate regulates leaf senescence and tolerance to cold stress: Crosstalk with other phytohormones. J Exp Bot **68**: 1361–1369

Hügler M, Sievert SM (2011) Beyond the Calvin Cycle: Autotrophic Carbon Fixation in the Ocean. Ann Rev Mar Sci **3**: 261–289

Ikegami A, Yoshimura N, Motohashi K, Takahashi S, Romano PGN, Hisabori T, Takamiya KI, Masuda T (2007) The CHLI1 subunit of Arabidopsis thaliana magnesium chelatase is a target protein of the chloroplast thioredoxin. J Biol Chem **282**: 19282–19291

Iqbal N, Khan NA, Ferrante A, Trivellini A, Francini A, Khan MIR (2017) Ethylene Role in Plant Growth, Development and Senescence: Interaction with Other Phytohormones. Front Plant Sci **8**: 1–19

Ishida H, Yoshimoto K, Izumi M, Reisen D, Yano Y, Makino A, Ohsumi Y, Hanson MR, Mae T (2008) Mobilization of Rubisco and Stroma-Localized Fluorescent Proteins of Chloroplasts to the Vacuole by an ATG Gene-Dependent Autophagic Process. Plant Physiol **148**: 142–155

Jansson S (1994) The light-harvesting chlorophyll ab-binding proteins. Biochim Biophys Acta - Bioenerg **1184**: 1–19

Järvi S, Suorsa M, Aro E-M (2015) Photosystem II repair in plant chloroplasts — Regulation, assisting proteins and shared components with photosystem II biogenesis. Biochim Biophys Acta - Bioenerg **1847**: 900–909

Jiang H, Li M, Liang N, Yan H, Wei Y, Xu X, Liu J, Xu Z, Chen F, Wu G (2007) Molecular cloning and function analysis of the stay green gene in rice. Plant J **52**: 197–209

Jibran R, Sullivan KL, Crowhurst R, Erridge ZA, Chagné D, McLachlan ARG, Brummell DA, Dijkwel PP, Hunter DA (2015) Staying green postharvest: how

three mutations in the Arabidopsis chlorophyll b reductase gene NYC1 delay degreening by distinct mechanisms. J Exp Bot. doi: 10.1093/jxb/erv390

John CF, Morris K, Jordan BR, Thomas B, A-H-Mackerness S (2001) Ultraviolet-B exposure leads to up-regulation of senescence-associated genes in Arabidopsis thaliana. J Exp Bot **52**: 1367–1373

Jordan DR, Hunt CH, Cruickshank AW, Borrell AK, Henzell RG (2012) The relationship between the stay-green trait and grain yield in elite sorghum hybrids grown in a range of environments. Crop Sci **52**: 1153–1161

Karim S, Aronsson H (2014) The puzzle of chloroplast vesicle transport â€“ involvement of GTPases. Front Plant Sci **5**: 1–12

Kato Y, Sun X, Zhang L, Sakamoto W (2012) Cooperative D1 Degradation in the Photosystem II Repair Mediated by Chloroplastic Proteases in Arabidopsis. Plant Physiol **159**: 1428–1439

Khan NZ, Lindquist E, Aronsson H (2013) New Putative Chloroplast Vesicle Transport Components and Cargo Proteins Revealed Using a Bioinformatics Approach: An Arabidopsis Model. PLoS One. doi: 10.1371/journal.pone.0059898

Komenda J, Sobotka R, Nixon PJ (2012) Assembling and maintaining the Photosystem II complex in chloroplasts and cyanobacteria. Curr Opin Plant Biol **15**: 245–251

Kondo K, Ochiai Y, Katayama M, Ikeuchi M (2007) The Membrane-Associated CpcG2-Phycobilisome in Synechocystis: A New Photosystem I Antenna. Plant Physiol **144**: 1200–1210

Kuai B, Chen J, Hörtensteiner S (2018) The biochemistry and molecular biology of chlorophyll breakdown. J Exp Bot **69**: 751–767

Kunugi M, Satoh S, Ihara K, Shibata K, Yamagishi Y, Kogame K, Obokata J, Takabayashi A, Tanaka A (2016) Evolution of Green Plants Accompanied Changes in Light-Harvesting Systems. Plant Cell Physiol **57**: 1231–1243

Kuras R, Wollman F-A (1994) The assembly of cytochrome b6/f complexes: an approach using genetic transformation of the green alga Chlamydomonas reinhardtii. EMBO J **13**: 1019–1027

Kusaba M, Tanaka A, Tanaka R (2013) Stay-green plants: what do they tell us about the molecular mechanism of leaf senescence. Photosynth Res **117**: 221–234

Leioatts N, Grubmüller H (2015) Understanding Thermodynamics of Conformational Change in the F-ATPase. Biophys J **108**: 58a

Leliaert F, Verbruggen H, Zechman FW (2011) Into the deep: New discoveries at the base of the green plant phylogeny. BioEssays **33**: 683–692

Li Z, Wu S, Chen J, Wang X, Gao J, Ren G, Kuai B (2017) NYEs/SGRs-mediated chlorophyll degradation is critical for detoxification during seed maturation in Arabidopsis. Plant J **92**: 650–661

Lim J, Paek N (2015) Quantitative Trait Locus Mapping and Candidate Gene Analysis for Functional Stay-Green Trait in Rice. **2015**: 95–107

Lim PO, Kim HJ, Nam HG, Gil Nam H (2007) Leaf Senescence. Annu Rev Plant Biol **58**: 115–136

Lin Y-P, Wu M-C, Charng Y (2016) Identification of a Chlorophyll Dephytylase Involved in Chlorophyll Turnover in Arabidopsis. Plant Cell **28**: 2974–2990

Lu Y (2016) Identification and Roles of Photosystem II Assembly, Stability, and Repair Factors in Arabidopsis. Front Plant Sci. doi: 10.3389/fpls.2016.00168

Luo PG, Deng KJ, Hu XY, Li LQ, Li X, Chen JB, Zhang HY, Tang ZX, Zhang Y, Sun QX, et al (2013a) Chloroplast ultrastructure regeneration with protection of photosystem II is responsible for the functional "stay-green" trait in wheat. Plant, Cell Environ **36**: 683–696

Luo Z, Zhang J, Li J, Yang C, Wang T, Ouyang B, Li H, Giovannoni J, Ye Z (2013b) A STAY-GREEN protein SlSGR1 regulates lycopene and β-carotene accumulation by interacting directly with SlPSY1 during ripening processes in tomato. New Phytol **198**: 442–452

Malnoe A, Wang F, Girard-Bascou J, Wollman F-A, de Vitry C (2014) Thylakoid FtsH Protease Contributes to Photosystem II and Cytochrome b6f Remodeling in Chlamydomonas reinhardtii under Stress Conditions. Plant Cell **26**: 373–390

Masclaux-Daubresse C, Purdy S, Lemaitre T, Pourtau N, Taconnat L, Renou J-P, Wingler A (2006) Genetic Variation Suggests Interaction between Cold Acclimation and Metabolic Regulation of Leaf Senescence. Plant Physiol **143**: 434–446

Matsuda K, Shimoda Y, Tanaka A, Ito H (2016) Chlorophyll a is a favorable substrate for Chlamydomonas Mg-dechelatase encoded by STAY-GREEN. Plant Physiol Biochem **109**: 365–373

Matsuo T, Okamoto K, Onai K, Niwa Y, Shimogawara K, Ishiura M (2008) A

systematic forward genetic analysis identified components of the Chlamydomonas circadian system. Genes Dev **22**: 918–930

Mayfield SP, Rahire M, Frank G, Zuber H, Rochaix JD (1987) Expression of the nuclear gene encoding oxygen-evolving enhancer protein 2 is required for high levels of photosynthetic oxygen evolution in Chlamydomonas reinhardtii. Proc Natl Acad Sci U S A **84**: 749–753

McNamara VP, Sutterwala FS, Whitmarsh J (1997) Structural model of cytochrome b559 in photosystem II based on a\rmutant with genetically fused subunits. Proc Natl Acad Sci U S A 1997 **94**: 14173–14178

Mellis A (1999) Photosystem-II damage and repair cycle in chloroplasts: What modulates the rate of photodamage in vivo? Trends Plant Sci **4**: 130–135

Miller JD, Arteca RN, Pell EJ (1999) Senescence-Associated Gene Expression during Ozone-Induced Leaf Senescence in Arabidopsis. Plant Physiol **120**: 1015–24

Minagawa J (2011) State transitions-the molecular remodeling of photosynthetic supercomplexes that controls energy flow in the chloroplast. Biochim Biophys Acta - Bioenerg **1807**: 897–905

Morita R, Sato Y, Masuda Y, Nishimura M, Kusaba M (2009) Defect in non-yellow coloring 3, an alpha/beta hydrolase-fold family protein, causes a stay-green phenotype during leaf senescence in rice. Plant J **59**: 940–952

Mozzo M, Dall'Osto L, Hienerwadel R, Bassi R, Croce R (2008) Photoprotection in the antenna complexes of photosystem II: Role of individual xanthophylls in chlorophyll triplet quenching. J Biol Chem **283**: 6184–6192

Mullet JE, Klein PG, Klein RR (1990) Chlorophyll regulates accumulation of the plastid-encoded chlorophyll apoproteins CP43 and D1 by increasing apoprotein stability. Proc Natl Acad Sci U S A **87**: 4038–4042

Mulo P, Sirpiö S, Suorsa M, Aro EM (2008) Auxiliary proteins involved in the assembly and sustenance of photosystem II. Photosynth Res **98**: 489–501

Murakami A, Miyashita H, Iseki M, Adachi K, Mimuro M (2004) Chlorophyll d in an Epiphytic Cyanobacterium of Red Algae. Science (80-) **303**: 1633

Murakami S, Kondo K, Katayama S, Hara S, Sunamura E-I, Yamashita E, Groth G, Hisabori T (2018) Structure of the γ-ε complex of cyanobacterial F1-ATPase reveals a suppression mechanism of the γ subunit on ATP-hydrolysis in phototrophs. Biochem J **85**: 2253–2266

Murchie EH, Lawson T (2013) Chlorophyll fluorescence analysis: a guide to good practice and understanding some new applications. J Exp Bot **64**: 3983–3998

Myouga F, Takahashi K, Tanaka RR, Nagata N, Kiss AZ, Funk C, Nomura Y, Nakagami H, Jansson S, Shinozaki K (2018) Stable accumulation of photosystem II requires ONE-HELIX PROTEIN1 (OHP1) of the light harvesting-like family. Plant Physiol **176**: pp.01782.2017

Neilson J, Durnford D (2010) Structural and functional diversification of the light-harvesting complexes in photosynthetic eukaryotes. Photosynth Res **106**: 57–71

Nelson N, Ben-Shem A (2004) The complex architecture of oxygenic photosynthesis. Nat Rev Mol Cell Biol **5**: 971–982

Nelson N, Ben-Shem A (2005) The structure of photosystem I and evolution of photosynthesis. BioEssays **27**: 914–922

Nelson N, Junge W (2015) Structure and Energy Transfer in Photosystems of Oxygenic Photosynthesis. Annu Rev Biochem **84**: 659–683

Nickelsen J, Rengstl B (2013) Photosystem II Assembly: From Cyanobacteria to Plants. Annu Rev Plant Biol **64**: 609–635

Nixon PJ, Michoux F, Yu J, Boehm M, Komenda J (2010) Recent advances in understanding the assembly and repair of photosystem II. Ann Bot **106**: 1–16

Ohad I, Kyle DJ, Arntzen CJ (1984) Membrane protein damage and repair: removal and replacement of inactivated 32-kilodalton polypeptides in chloroplast membranes. J Cell Biol **99**: 481–485

Ohnishi N, Takahashi Y (2001) PsbT Polypeptide Is Required for Efficient Repair of Photodamaged Photosystem II Reaction Center. J Biol Chem **276**: 33798–33804

Park S, Khamai P, Garcia-Cerdan JG, Melis A (2007a) REP27, a Tetratricopeptide Repeat Nuclear-Encoded and Chloroplast-Localized Protein, Functions in D1/32-kD Reaction Center Protein Turnover and Photosystem II Repair from Photodamage. Plant Physiol **143**: 1547–1560

Park SY, Yu JW, Park JS, Li J, Yoo SC, Lee NY, Lee SK, Jeong SW, Seo HS, Koh HJ, et al (2007b) The senescence-induced staygreen protein regulates chlorophyll degradation. Plant Cell **19**: 1649–1664

Peng L (2006) LOW PSII ACCUMULATION1 Is Involved in Efficient Assembly of Photosystem II in Arabidopsis thaliana. Plant Cell Online **18**: 955–969

Pi X, Tian L, Dai H-E, Qin X, Cheng L, Kuang T, Sui S-F, Shen J-R (2018)

Unique organization of photosystem I–light-harvesting supercomplex revealed by cryo-EM from a red alga. Proc Natl Acad Sci 201722482

Pruzinska A, Tanner G, Anders I, Roca M, Hörtensteiner S, Hortensteiner S (2003) Chlorophyll breakdown: pheophorbide a oxygenase is a Rieske-type iron-sulfur protein, encoded by the accelerated cell death 1 gene. Proc Natl Acad Sci U S A **100**: 15259–15264

Qian L, Voss-Fels K, Cui Y, Jan HU, Samans B, Obermeier C, Qian W, Snowdon RJ (2016) Deletion of a Stay-Green Gene Associates with Adaptive Selection in Brassica napus. Mol Plant **9**: 1559–1569

Qin X, Suga M, Kuang T, Shen J-R (2015) Structural basis for energy transfer pathways in the plant PSI-LHCI supercomplex. Science (80-) **348**: 989–995

Rantala M, Tikkanen M, Aro E-M (2017) Proteomic characterization of hierarchical megacomplex formation in Arabidopsis thylakoid membrane. Plant J **92**: 951–962

Ren G, An K, Liao Y, Zhou X, Cao Y, Zhao H, Ge X, Kuai B (2007) Identification of a Novel Chloroplast Protein AtNYE1 Regulating Chlorophyll Degradation during Leaf Senescence in Arabidopsis. Plant Physiol **144**: 1429–1441

Rev A, Physiol P, Mol P, Downloaded B (2000) T He C Hloroplast Atp S Ynthase : Structure 83–109

Rokka A, Suorsa M, Saleem A, Battchikova N, Aro E (2005) Synthesis and assembly of thylakoid protein complexes : multiple assembly steps of photosystem II. **168**: 159–168

Rong H, Tang Y, Zhang H, Wu P, Chen Y, Li M, Wu G, Jiang H (2013) The Stay-Green Rice like (SGRL) gene regulates chlorophyll degradation in rice. J Plant Physiol **170**: 1367–1373

Rossi S, Burgess P, Jespersen D, Huang B (2017) Heat-induced leaf senescence associated with chlorophyll metabolism in bentgrass lines differing in heat tolerance. Crop Sci **57**: S-169-S-178

Saga Y, Hirai Y, Sadaoka K, Isaji M, Tamiaki H (2013) Structure-Dependent Demetalation Kinetics of Chlorophyll a Analogs under Acidic Conditions. Photochem Photobiol **89**: 68–73

Sakuraba Y, Kim D, Kim Y-S, Hörtensteiner S, Paek N-C (2014) Arabidopsis STAYGREEN-LIKE (SGRL) promotes abiotic stress-induced leaf yellowing during vegetative growth. FEBS Lett **588**: 3830–3837

Sakuraba Y, Schelbert S, Park S-Y, Han S-H, Lee B-DB-D, Andrès CB, Kessler F, Hörtensteiner S, Paek N-CN-C, Andres CB, et al (2012) STAY-GREEN and Chlorophyll Catabolic Enzymes Interact at Light-Harvesting Complex II for Chlorophyll Detoxification during Leaf Senescence in Arabidopsis. Plant Cell **24**: 507–518

Sakuraba Y, Yamasato A, Tanaka R, Tanaka A (2007) Functional analysis of N-terminal domains of Arabidopsis chlorophyllide a oxygenase. Plant Physiol Biochem **45**: 740–749

Sato T, Shimoda Y, Matsuda K, Tanaka A, Ito H (2018) Mg-dechelation of chlorophyll a by Stay-Green activates chlorophyll b degradation through expressing Non-Yellow Coloring 1 in Arabidopsis thaliana. J Plant Physiol **222**: 94–102

Sato Y, Morita R, Nishimura M, Yamaguchi H, Kusaba M (2007) Mendel's green cotyledon gene encodes a positive regulator of the chlorophyll-degrading pathway. Proc Natl Acad Sci U S A **104**: 14169–14174

Schelbert S, Aubry S, Burla B, Agne B, Kessler F, Krupinska K, Hortensteiner S (2009) Pheophytin Pheophorbide Hydrolase (Pheophytinase) Is Involved in Chlorophyll Breakdown during Leaf Senescence in Arabidopsis. Plant Cell Online **21**: 767–785

Schmollinger S, Muhlhaus T, Boyle NR, Blaby IK, Casero D, Mettler T, Moseley JL, Kropat J, Sommer F, Strenkert D, et al (2014) Nitrogen-Sparing Mechanisms in Chlamydomonas Affect the Transcriptome, the Proteome, and Photosynthetic Metabolism. Plant Cell **26**: 1410–1435

Schulz-Raffelt M, Chochois V, Auroy P, Cuiné S, Billon E, Dauvillée D, Li-Beisson Y, Peltier G (2016) Hyper-accumulation of starch and oil in a Chlamydomonas mutant affected in a plant-specific DYRK kinase. Biotechnol Biofuels **9**: 1–12

Sembdner G, Parthier B (1993) The Biochemistry and the Physiological and Molecular Actions of Jasmonates. Annu Rev Plant Physiol Plant Mol Biol **44**: 569–589

Sharma SK, Nelson DR, Abdrabu R, Khraiwesh B, Jijakli K, Arnoux M, O'Connor MJ, Bahmani T, Cai H, Khapli S, et al (2015) An integrative Raman microscopy-based workflow for rapid in situ analysis of microalgal lipid bodies. Biotechnol Biofuels **8**: 1–14

Shen J-R (2015) The Structure of Photosystem II and the Mechanism of Water Oxidation in Photosynthesis. Annu Rev Plant Biol **66**: 23–48

Shimoda Y, Ito H, Tanaka A (2012) Conversion of chlorophyll b to chlorophyll a precedes magnesium dechelation for protection against necrosis in Arabidopsis. Plant J **72**: 501–511

Shimoda Y, Ito H, Tanaka A (2016) Arabidopsis *STAY-GREEN* , Mendel's Green Cotyledon Gene, Encodes Magnesium-Dechelatase. Plant Cell **28**: 2147–2160

Singh NP, Vaishali (2016) Characterization of wheat (Triticum aestivum) for stay green trait. J Appl Nat Sci **8**: 107–111

Sirpiö S, Khrouchtchova A, Allahverdiyeva Y, Hansson M, Fristedt R, Vener A V., Scheller HV, Jensen PE, Haldrup A, Aro EM (2008) AtCYP38 ensures early biogenesis, correct assembly and sustenance of photosystem II. Plant J **55**: 639–651

Storf S, Jansson S, Schmid VHR (2005) Pigment binding, fluorescence properties, and oligomerization behavior of Lhca5, a novel light-harvesting protein. J Biol Chem **280**: 5163–5168

Sunku K, De Groot HJM, Pandit A (2013) Insights into the photoprotective switch of the major light-harvesting complex II (LHCII): A preserved core of arginine-glutamate interlocked helices complemented by adjustable loops. J Biol Chem **288**: 19796–19804

Swiatek M, Regel RE, Meurer J, Wanner G, Pakrasi HB, Ohad I, Herrmann RG (2003) Effects of selective inactivation of individual genes for low-molecular-mass subunits on the assembly of photosystem II, as revealed by chloroplast transformation: the $psbEFLJ$ operon in \textit{Nicotiana tabacum}. Mol Genet Genomics **268**: 699–710

Sztatelman O, Grzyb J, Gabryś H, Banaś AK (2015) The effect of UV-B on Arabidopsis leaves depends on light conditions after treatment. BMC Plant Biol **15**: 1–16

Takabayashi A, Kurihara K, Kuwano M, Kasahara Y, Tanaka R, Tanaka A (2011) The oligomeric states of the photosystems and the light-harvesting complexes in the Chl b-less mutant. Plant Cell Physiol **52**: 2103–2114

Tanaka A, Ito H, Tanaka R, Tanaka NK, Yoshida K, Okada K (1998) Chlorophyll a oxygenase (CAO) is involved in chlorophyll b formation from chlorophyll a. Proc Natl Acad Sci U S A **95**: 12719–12723

Tanaka A, Yamamoto Y, Tsuji H (1991) Formation of chlorophyll-protein complexes during greening 2. Redistribution of chlorophyll among apoproteins. Plant Cell Physiol **32**: 195–204

Tanz SK, Kilian J, Johnsson C, Apel K, Small I, Harter K, Wanke D, Pogson B, Albrecht V (2012) The SCO2 protein disulphide isomerase is required for thylakoid biogenesis and interacts with LCHB1 chlorophyll a/b binding proteins which affects chlorophyll biosynthesis in Arabidopsis seedlings. Plant J **69**: 743–754

Theis J, Schroda M (2016) Revisiting the photosystem II repair cycle. Plant Signal Behav **11**: 1–8

Thomas H, Howarth CJ (2000) Five ways to stay green. J Exp Bot **51**: 329–337

Thomas H, Ougham H (2014) The stay-green trait. J Exp Bot **65**: 3889–3900

Thomas H, Ougham H, Canter P, Donnison I (2002) What stay-green mutants tell us about nitrogen remobilization in leaf senescence. J Exp Bot **53**: 801–808

THOMAS H, SMART CM (1993) Crops that stay green. Ann Appl Biol **123**: 193–219

Torabi S, Umate P, Manavski N, Plöchinger M, Kleinknecht L, Bogireddi H, Herrmann RG, Wanner G, Schröder WP, Meurer J (2014) PsbN Is Required for Assembly of the Photosystem II Reaction Center in Nicotiana tabacum. Plant Cell Online **26**: 1183–1199

Umena Y, Kawakami K, Shen JR, Kamiya N (2011) Crystal structure of oxygen-evolving photosystem II at a resolution of 1.9 A. Nature **473**: 55–60

Uniacke J, Zerges W (2007) Photosystem II Assembly and Repair Are Differentially Localized in Chlamydomonas. Plant Cell Online **19**: 3640–3654

Vavilin D, Vermaas W (2007) Continuous chlorophyll degradation accompanied by chlorophyllide and phytol reutilization for chlorophyll synthesis in Synechocystis sp. PCC 6803. Biochim Biophys Acta - Bioenerg **1767**: 920–929

Version D (2008) University of Groningen Molecular aspects of ageing and the onset of leaf senescence Schippers, Jozefus Hendrikus Maria. 6–12

Wan T, Li M, Zhao X, Zhang J, Liu Z, Chang W (2014) Crystal structure of a multilayer packed major light-harvesting complex: Implications for grana stacking in higher plants. Mol Plant **7**: 916–919

Wang F, Qi Y, Malnoë A, Choquet Y, Wollman FA, de Vitry C (2017) The High Light Response and Redox Control of Thylakoid FtsH Protease in

Chlamydomonas reinhardtii. Mol Plant **10**: 99–114

Watanabe M, Semchonok DA, Webber-Birungi MT, Ehira S, Kondo K, Narikawa R, Ohmori M, Boekema EJ, Ikeuchi M (2014) Attachment of phycobilisomes in an antenna-photosystem I supercomplex of cyanobacteria. Proc Natl Acad Sci **111**: 2512–2517

Wientjes E, Croce R (2011) The light-harvesting complexes of higher-plant Photosystem I: Lhca1/4 and Lhca2/3 form two red-emitting heterodimers. Biochem J **433**: 477–485

Wingler A, Roitsch T (2008) Metabolic regulation of leaf senescence: Interactions of sugar signalling with biotic and abiotic stress responses. Plant Biol **10**: 50–62

Wu S, Li Z, Yang L, Xie Z, Chen J, Zhang W, Liu T, Gao S, Gao J, Zhu Y, et al (2016) NON-YELLOWING2 (NYE2), a close paralog of NYE1, plays a positive role in chlorophyll degradation in Arabidopsis. Mol Plant **9**: 624–627

Xu W, Subudhi PK, Crasta OR, Rosenow DT, Mullet JE, Nguyen HT (2000) Molecular mapping of QTLs conferring stay-green in grain sorghum (Sorghum bicolor L. Moench). Genome **43**: 461–469

Yang D-H, Webster J, Adam Z, Lindahl M, Andersson B (1998) Induction of Acclimative Proteolysis of the Light-Harvesting Chlorophyll a/b Protein of Photosystem II in Response to Elevated Light Intensities. Plant Physiol **118**: 827–834

Yasuhito S, So-Yon P, and Nam-Chon P (2015) The Divergent Roles of STAYGREEN (SGR) Homologs in Chlorophyll Degradation. Mol Cells **38**: 390–395

Yokono M, Takabayashi A, Akimoto S, Tanaka A (2015) A megacomplex composed of both photosystem reaction centres in higher plants. Nat Commun **6**: 1–6

Yoo SC, Cho SH, Zhang H, Paik HC, Lee CH, Li J, Yoo JH, Lee BW, Koh HJ, Seo HS, et al (2007) Quantitative trait loci associated with functional stay-green SNU-SG1 in rice. Mol Cells **24**: 83–94

Yu J, Knoppová J, Michoux F, Bialek W, Cota E, Shukla MK, Strašková A, Pascual Aznar G, Sobotka R, Komenda J, et al (2018) Ycf48 involved in the biogenesis of the oxygen-evolving photosystem II complex is a seven-bladed beta-propeller protein. Proc Natl Acad Sci **115**: E7824–E7833

Zabelin AA, Shkuropatova VA, Makhneva ZK, Moskalenko AA, Shuvalov VA,

Shkuropatov AY (2014) Chemically modified reaction centers of photosystem II: Exchange of pheophytin a with 7-deformyl-7-hydroxymethyl-pheophytin b. Biochim Biophys Acta - Bioenerg **1837**: 1870–1881

Zhang K, Halitschke R, Yin C, Liu C-J, Gan S-S (2013) Salicylic acid 3-hydroxylase regulates *Arabidopsis* leaf longevity by mediating salicylic acid catabolism. Proc Natl Acad Sci **110**: 14807–14812

Zhang S, Frankel LK, Bricker TM (2010) The Sll0606 protein is required for photosystem II assembly/stability in the cyanobacterium Synechocystis sp. PCC 6803. J Biol Chem **285**: 32047–32054

Zhou C, Han L, Pislariu C, Nakashima J, Fu C, Jiang Q, Quan L, Blancaflor EB, Tang Y, Bouton JH, et al (2011) From Model to Crop: Functional Analysis of a STAY-GREEN Gene in the Model Legume Medicago truncatula and Effective Use of the Gene for Alfalfa Improvement. Plant Physiol **157**: 1483–1496

Zhu X, Chen J, Qiu K, Kuai B (2017) Phytohormone and Light Regulation of Chlorophyll Degradation. Front Plant Sci. doi: 10.3389/fpls.2017.01911

Acknowledgments

I would like to sincere gratitude to my supervisor Professor Ayumi Tanaka for giving me this precious opportunity to conduct this research, and for his constant support and valuable guidance throughout my studies.

I would also like to thank my co-supervisor professor assistant Professor Hisashi Ito and professor Tomomichi Fujita granting me the opportunity to utilize the excellent facilities available in the laboratory and for their constant support, guidance, and encouragement during my whole research.

I wish to express my gratitude to associate professor Ryouichi Tanaka and assistant Professor Atsushi Takabayashi for their teaching and helping. I also wish to extend my deeply appreciate to all the members of the plant adaptation biology group.

I would like to thank the Ministry of Education, Culture, Sports, Science and Technology of Japan and the China Scholarship Council.

Lastly, I would like to thank my family and friends for their unwavering support and understanding throughout my studies.